© 2025 Journal of Pharmacy & Pharmacognosy Research, 13 (6), 1649-1677, 2025
ISSN 0719-4250
https://jppres.com

DOI: https://doi.org/10.56499/jppres24.2213_13.6.1649

Original Article

Phytochemical analysis of *Passiflora quadrangularis* L. and its potential role in hypertension and cardiac remodeling

[Análisis fitoquímico de *Passiflora quadrangularis* L. y su posible papel en la hipertensión y el remodelado cardíaco]

Lesly L. Bareño[1], Pilar Puebla[2,4], María J. Montero[3,4], María A. Sevilla[3,4], Mario F. Guerrero[1*], Arturo San Feliciano[2,5]

[1]Department of Pharmacy, Universidad Nacional de Colombia, Bogotá D.C, 111321, Colombia.
[2]Department of Pharmaceutical Sciences, Universidad de Salamanca, Salamanca, 37007, Spain.
[3]Department of Physiology and Pharmacology, Universidad de Salamanca, Salamanca, 37007, Spain.
[4]Biomedical Research Institute of Salamanca (IBSAL), Hospital Virgen de la Vega, Salamanca, 37007, Spain.
[5]Postgraduate Programme in Pharmaceutical Sciences, Universidade do Vale do Itajaí, Itajaí, 88302-901, Brazil.
*E-mail: mfquerrerop@unal.edu.co

Abstract

Context: Hypertension is a major risk factor for cardiovascular disease and stroke, contributing significantly contributing to increased morbidity and premature mortality worldwide. Further research into new treatments and the pathophysiology of this disease is necessary.

Aims: To isolate and identify bioactive fractions and compounds from *Passiflora quadrangularis* L., and to evaluate their antihypertensive and anti-remodeling effects in rat models.

Methods: The *P. quadrangularis* extract was fractionated and analyzed through chromatographic and spectroscopic techniques. Various fractions and the total extract were used to treat spontaneously hypertensive rats (SHRs), whose blood pressure was measured weekly using a non-invasive method. Vascular reactivity assays were then performed, and morphometric and morphological parameters were calculated. In Wistar rats, vascular reactivity assays were performed using isolated fractions and compounds.

Results: Nine compounds were isolated in the phytochemical analysis. Evaluation of the antihypertensive effect of the treatments revealed significant differences versus the control group. Concentration–response curves of all treatments shifted along the concentration axis, indicating improved EC_{50} values, with significant differences compared to the control group in both SHRs and Wistar rats. Histological analysis revealed a reduction in cardiac and vascular fibrosis across all treatment groups.

Conclusions: Phytochemical analysis identified novel compounds for *P. quadrangularis. In vivo* studies utilizing SHRs revealed that *P. quadrangularis* extract and its fractions significantly attenuated systolic blood pressure, improved endothelium-dependent relaxation, and mitigated cardiac hypertrophy and vascular remodeling. Organ bath assays suggested the involvement of multiple pathways, including NO-cGMP signaling, activation of K^+ channels, and modulation of adrenergic and muscarinic receptors.

Keywords: blood pressure; hypertension; hypertrophy; spontaneously hypertensive rats; vascular remodeling.

Resumen

Contexto: La hipertensión es el mayor factor de riesgo crítico para las enfermedades cardiovasculares y los accidentes cerebrovasculares, contribuyendo significativamente al incremento de la morbilidad y mortalidad prematura a nivel mundial. Es necesario continuar investigando nuevos tratamientos y avanzar en el estudio de la fisiopatología de esta enfermedad.

Objetivos: Aislar e identificar fracciones y compuestos bioactivos de *Passiflora quadrangularis* L. y evaluar sus efectos antihipertensivo y anti-remodelado en ratas.

Métodos: El extracto de *P. quadrangularis* fue fraccionado y analizado mediante técnicas cromatográficas y espectroscópicas. Se utilizaron diversas fracciones y el extracto total para tratar ratas espontáneamente hipertensas, a las que se les midió la presión arterial semanalmente mediante un método no invasivo. Luego se realizaron pruebas de funcionalidad de los órganos y se calcularon parámetros morfométricos y morfológicos. En ratas Wistar, se evaluó la reactividad vascular con las fracciones y compuestos obtenidos.

Resultados: En el análisis fitoquímico se aislaron nueve compuestos. La evaluación del efecto antihipertensivo de los tratamientos reveló diferencias significativas versus el control. Las curvas de concentración-respuesta de todos los tratamientos se desplazaron a lo largo del eje de concentración, lo que indica una mejora en los valores de EC_{50}, con diferencias significativas en comparación con el grupo control, tanto en ratas SHR como en ratas Wistar. El análisis histológico reveló una reducción de la fibrosis cardíaca y vascular en todos los grupos tratados.

Conclusiones: El análisis fitoquímico identificó nuevos compuestos para *P. quadrangularis*. Los estudios *in vivo* utilizando SHRs revelaron que el extracto de *P. quadrangularis* y sus fracciones atenuaron significativamente la presión arterial sistólica, mejoraron la relajación dependiente del endotelio y mitigaron la hipertrofia cardíaca y la remodelación vascular. El ensayo del baño de órganos sugirió que la participación de vías como la señalización NO-GMPc, la activación de los canales de K^+ y la modulación de los receptores adrenérgicos y muscarínicos podrían estar implicadas.

Palabras Clave: hipertensión; hipertrofia; presión arterial; ratas espontáneamente hipertensas; remodelación vascular.

ARTICLE INFO
Received: September 21, 2024.
Accepted: June 27, 2025.
Available Online: August 13, 2025.

AUTHOR INFO
ORCID: 0000-0003-3205-6976 (LLB) 0000-0003-2125-0378 (MJM)
0000-0003-1789-1818 (MFG) 0000-0003-2960-8514 (MAS)
0000-0003-2623-1256 (PP) 0000-0002-0578-0611 (ASF)

Abbreviations: ACh: acetylcholine; CH: cardiac hypertrophy; CH_2Cl_2: dichloromethane; Coll-I: collagen type I; Coll-III: collagen type III; DEPT: distortionless enhancement by polarization transfer; DF: dichloromethane fraction; DMSO: dimethyl sulfoxide; EC_{50}: effective concentration of 50%; EtOAc: ethyl acetate; HMBC: heteronuclear multiple bond correlation; HRMS: high resolution mass spectrometry; HSQC: heteronuclear single quantum coherence; KPSS: potassium salt solution; L-NAME: N(G)-nitro-L-arginine methyl ester; MeOH: methanol; MF: methanol fraction; NO: nitric oxide; NOS: nitric oxide synthase; ODQ: 1H-[1,2,4] oxadiazole [4,3-a]quinoxalin-1-one; PE: phenylephrine; ROS: reactive oxygen species; SBP: systolic blood pressure; sGC: soluble guanylyl cyclase; SHR: spontaneously hypertensive rat; SNP: sodium nitroprusside; TMS: tetramethylsilane; VPR: volume pressure recording; VSMCs: vascular smooth muscle cells; W_{IVS}/R: interventricular septum thickness/heart radius ratio; W_{LV}/R: left ventricular thickness/heart radius ratio.

INTRODUCTION

Hypertension is a leading risk factor for cardiovascular diseases and stroke (Boateng and Ampofo, 2023). It remains one of the most prevalent causes of premature morbidity and mortality worldwide (Hawlitschek et al., 2022; Lozano et al., 2012). The most common form, essential hypertension, is a complex and multifactorial condition influenced by both genetic predisposition and environmental factors.

Hypertension and cardiac pressure overload contribute to cardiac hypertrophy, increased vascular resistance, morphological alterations in vascular smooth muscle cells (VSMCs), and fibrosis, primarily due to the accumulation of type I (Coll-I) and type III (Coll-III) collagen (Gao et al., 2012; Hawlitschek et al., 2022; Kokubo et al., 2005; Yang et al., 1997). Additionally, hypertension induces endothelial dysfunction by reducing nitric oxide (NO) bioavailability (Zanetti et al., 2010) and promoting an overproduction of reactive oxygen species (ROS) (Fiorim et al., 2012).

Herbal medicinal plants are widely used to treat various pathological conditions and represent an inexhaustible source of bioactive compounds. The genus *Passiflora* comprises approximately 500 species, predominantly distributed across Central and South America (Dhawan et al., 2004). The highest species diversity is found in Colombia, Brazil, Ecuador, and Peru (Sepúlveda et al., 2018).

Various ethnopharmacological uses have been attributed to the *Passiflora* genus, including anxiolytic, anti-inflammatory, and antidiabetic effects, as well as protective properties against cardiovascular diseases (Castro et al., 2007; Dhawan et al., 2004; Martos et al., 2020). Previous studies have shown that extracts of *Passiflora quadrangularis* L. may aid in the management of hypertension and the prevention of vascular remodeling (Bareño et al., 2017; Dhawan et al., 2004).

The aim of this study was to isolate novel compounds from the ethanolic extract of *P. quadrangularis* leaves and to evaluate the antihypertensive and anti-remodeling effects of the isolated fractions using both *in vivo* and in *vitro* models.

MATERIAL AND METHODS

Extraction and fractionation

Plant material from *P. quadrangularis* was collected from the municipality of Algeciras in the Huila Department, Colombia (latitude 2.54750; longitude -75.28727). This area has an elevation of 1100 MASL and an average temperature of 24°C. Voucher specimens were deposited at the Colombian National Herbarium (Code N° COL 602879). The leaves of *P. quadrangularis* were dried at 40°C in a circulating air oven; the dried material was ground and percolated with ethanol for 72 hours, then filtered and concentrated with a rotary evaporator.

The ethanolic extract was dissolved in methanol and stored at -18°C for 12 hours until the wax precipitated. The wax-free extract was separated into two fractions with dichloromethane (CH_2Cl_2) and methanol (MeOH) in different proportions (8:2 and 8.5:1.5, respectively), thus obtaining DF and MF.

Isolation and structural elucidation

The DF was further fractionated by flash column chromatography. The elution system was selected based on preliminary thin-layer chromatography (TLC) analysis, using hexane, ethyl acetate (EtOAc), and MeOH as solvents. Silica gel 60 (particle size 0.040–0.063 mm; Merck 13) was used as the stationary phase, and the mobile phase was applied with increasing polarity. A total of 24 fractions (15 mL each) were collected based on their TLC profiles. This procedure led to the isolation of nine pure compounds from subfractions DF-1 to DF-7, as well as a compound mixture (DF-8) (Fig. 1).

TLC analysis was performed to compare the MF, DF, and the crude ethanolic extract, using a hexane: EtOAc (8:2) solvent system. The MF was found to be rich in flavonoids and cycloartanolic saponins. Based on these results, compound isolation efforts were focused on the DF.

High-resolution mass spectrometry (HRMS) was performed using a QSTAR XL spectrometer (Applied Biosystems). UV spectra were recorded with a Spectrum BX FTIR spectrophotometer (PerkinElmer). Melting points were determined using a Gallenkamp

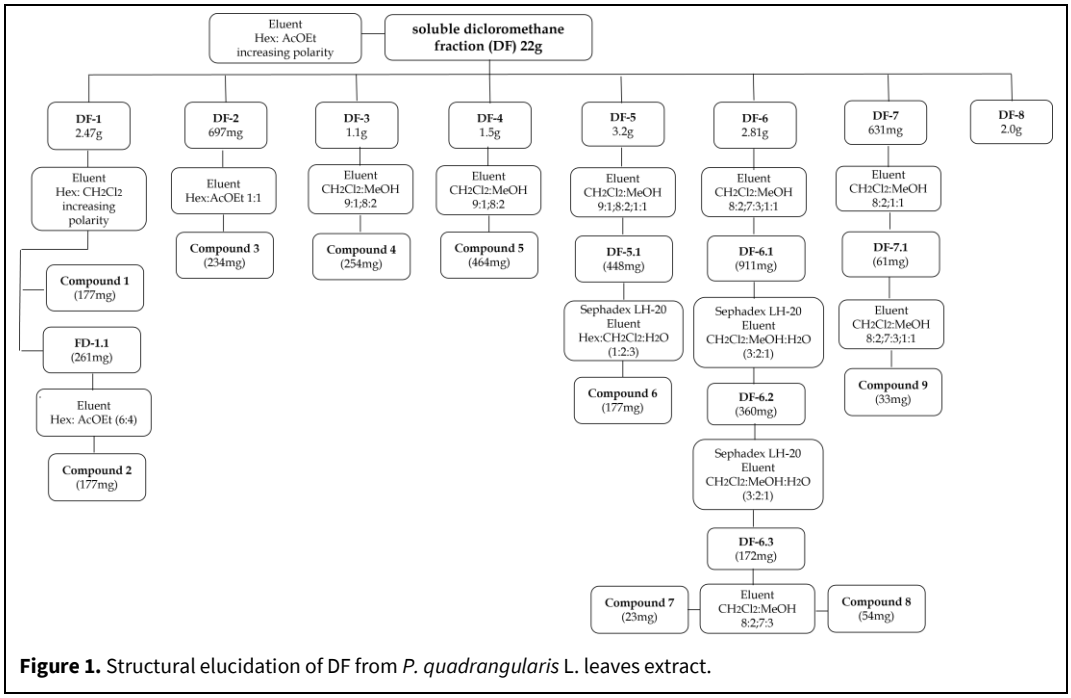

Figure 1. Structural elucidation of DF from *P. quadrangularis* L. leaves extract.

electronic melting point apparatus. Nuclear magnetic resonance (NMR) spectra (^{1}H and ^{13}C) were acquired on a Bruker DRX-400 spectrometer. Chemical shifts (δ) are reported in parts per million (ppm) relative to tetramethylsilane (TMS) as the internal standard and coupling constants (*J*) are given in Hertz (Hz).

Experimental design using spontaneously hypertensive rats

All experiments were performed according to the European Union directives for the ethical care and use of laboratory animals (Register 308 of 2018). Twenty male 11-week-old spontaneously hypertensive rats (SHRs) were supplied by Elevage Janvier, Le Genest-Saint-Isle, France, and maintained at a temperature of 23°C with a 12-hour light/dark cycle. The animals were acclimated for one week and then were randomly divided into four groups of 5. The control group (C) received no treatment, while the other groups received one of the following treatments for six weeks: total extract of *P. quadrangularis* (E), soluble fraction in MeOH (MF), and soluble fraction in CH_2Cl_2 (DF). The treatments were administered mixed with the rats' standard solid diet, formulated to provide 75 mg/kg of body weight per day. The animals had *ad libitum* access to water. The rats' body weight and daily food intake were estimated weekly.

Systolic blood pressure measurement

Systolic blood pressure (SBP) was measured using the non-invasive tail-cuff method with a CODA monitor system (Kent Scientific, USA). Rats were placed in restrainers and maintained at a constant temperature of 38°C for 10–15 minutes to induce vasodilation in the tail artery. Subsequently, the occlusion cuff and the volume pressure recording (VPR) sensor cuff were positioned at the base of the tail. Measurements were performed at the same time each day (between 09:00 and 13:00) to minimize circadian variability. SBP values were calculated as the average of 10 consecutive readings (Sánchez et al., 2011).

Organ bath preparation

At the end of the treatment period, animals were anesthetized with sodium pentobarbital (60 mg/kg body weight, i.p.) and euthanized by exsanguination. The heart, aorta, and mesenteric vascular bed were immediately excised and placed in ice-cold Krebs solution (composition in mM: NaCl 118, KCl 4.7, $CaCl_2$ 2.5, KH_2PO_4 1.2, $MgSO_4 \cdot 7H_2O$ 1.2, $NaHCO_3$ 25, glucose 11; pH 7.4). Tissues were then processed accordingly for subsequent functional studies.

Aortic ring experiments: the descending thoracic aorta was dissected by thoracotomy and immersed in ice-cold Krebs solution for preservation. The surrounding aortic tissue was removed, and fragments were cut into 3 mm lengths. Thoracic aortic rings were connected using an isometric force transducer (UF1, Harvard Apparatus Inc., USA), submerged in Allhin organ chambers containing 5 mL of Krebs solution maintained at 37°C, and continuously exposed to a carbogen mixture of 95% O_2 and 5% CO_2. Force was recorded on a computer using LabChart version 3.4 software and a PowerLab/800 data acquisition system (AD Instruments, UK).

A basal tension of 2 g was applied to each aortic ring with a stabilization period of 60 minutes. The

Krebs solution was periodically changed, and tension was reset during this period. Once equilibrium was reached, the aortic rings were exposed to a high potassium salt solution (KPSS) to assess tissue functionality. After a washout period, phenylephrine (PE, 0.1 µM) was added to achieve a steady state of tissue precontraction, and concentrations of acetylcholine (ACh, 10^{-8} to 10^{-4} M) or sodium nitroprusside (SNP, 10^{-8} to 10^{-5} M) were added to induce relaxation. The PE cumulative concentration-response curves (10^{-8} to 10^{-4} M) were also evaluated.

Mesenteric ring experiments: The third-order branch of the mesenteric arterial bed was carefully dissected, and surrounding connective tissue was removed. The vessel was then cut into 2 mm-long segments and mounted in a small-vessel dual-chamber myograph system (DMT A/S, Denmark) for isometric tension recording. Two stainless steel wires (40 µm in diameter) were inserted through the lumen of each segment to secure them in the myograph chambers, as previously described (Sánchez et al., 2011).

Following a 30-minute equilibration period in Krebs solution (bubbled with carbogen, 95% O_2/5% CO_2) at 37°C and pH 7.4, mesenteric segments were stretched to their optimal lumen diameter for active tension development. After an additional 30-minute stabilization period, vessels were exposed to high-potassium physiological salt solution (KPSS) to assess contractile responsiveness. Following a washout and a further 15-minute equilibration, segments were precontracted with phenylephrine (PE, 3 µM). Once a stable maximal contraction was achieved, cumulative concentration–response curves were generated for ACh (10^{-8} to 10^{-5} M) or SNP (10^{-8} to 10^{-5} M). PE concentration–response curves (10^{-8} to 10^{-4} M) were also evaluated. Segments exhibiting less than 50% relaxation in response to ACh were excluded from analysis.

Cardiac and vascular hypertrophy and fibrosis

Heart: The atria were removed, and all epicardial fat was carefully dissected before weighing the heart. The cardiac hypertrophy (CH) index was calculated as the ratio of heart weight to body weight. A transverse section of the heart was fixed in 4% formaldehyde, embedded in paraffin, and sectioned at a thickness of 4 µm for histological analysis.

Tissue sections were stained with Sirius Red, a collagen-specific dye. Images from at least five distinct areas of each heart were captured using the Image J software. Morphometric measurements were performed in duplicate by the same observer. The following parameters were calculated: the ratio of left ventricular wall thickness to heart radius (W_{LV}/R) and the ratio of interventricular septum thickness to heart radius (W_{IVS}/R).

Collagen content was quantified using Adobe Photoshop CS2 (Microsoft®) by calculating the percentage of interstitial fibrosis in each image. This was determined as the ratio of the collagen-stained area to the total myocardial surface area.

Aorta: Cleaned aortic rings were embedded in paraffin and sectioned at a thickness of 4 µm. Sections were stained with Masson's trichrome, a collagen-specific histological stain. Images from at least three distinct areas of each aortic section were captured using the Image J software for subsequent analysis.

To obtain morphometric parameters, each measurement was performed in duplicate by the same observer. The cross-sectional area of the tunica media (CSA_m) was calculated using the formula [1].

$$CSA_m = A_e - A_i \quad [1]$$

where: A_e = external area, A_i = internal area, W_m = tunica media thickness, L = lumen diameter. The wall-to-lumen ratio (W_m/L) was also determined.

Collagen content was quantified using Adobe Photoshop CS2 (Microsoft®). The percentage of interstitial fibrosis for each image was calculated as the ratio of the collagen-stained area to the total vascular surface area.

Experimental design using Wistar rats

All procedures were conducted in accordance with the ethical guidelines for the care and use of laboratory animals established by the Ethics Committee of the Universidad Nacional de Colombia (Act 013 of 2017). Twenty male Wistar rats (200–300 g) were provided by the Department of Pharmacy, Universidad Nacional de Colombia, and maintained under the previously described housing conditions. Aortic rings from these animals were used to evaluate the vasodilatory effects of the DF, subfraction DF-8, and compound **6**, as well as the vasoconstrictor effect of the MF.

Aortic ring experiments

Animals were euthanized using a CO_2 chamber. The descending thoracic aorta was carefully dissected via thoracotomy and immediately immersed in ice-cold Krebs solution for preservation. Surrounding connective tissue was removed, and the aorta was cut into 3 mm-long rings. Each ring was mounted on an isometric force transducer and suspended in Allhin organ chambers containing 5 mL of Krebs solution, maintained at 37°C and continuously aerated with a carbogen mixture (95% O_2 and 5% CO_2). Isometric tension was recorded using LabTrax software and a

data acquisition system from World Precision Instruments (WPI, USA).

A resting tension of 2 g was applied to each aortic ring, followed by a 60-minute stabilization period during which the Krebs solution was refreshed periodically, and baseline tension was readjusted as needed. Once equilibrium was achieved, phenylephrine (PE, 1 µM) was added to induce a stable contractile response. Subsequently, cumulative concentrations of acetylcholine (ACh, 10^{-8} to 10^{-4} M) were administered to assess endothelial integrity. Rings exhibiting less than 70% relaxation were excluded from further analysis.

The rings were then washed with fresh Krebs solution for an additional hour, with periodic solution changes and tension readjusted to 2 g. After re-establishing a stable baseline, PE (1 µM) was re-administered to induce precontraction. Once a steady contractile plateau was reached, cumulative concentrations of DF-8, DF, and compound **6** (1–300 µg/mL) were added to evaluate their vasorelaxant effects.

To evaluate the mechanism of action, antagonists targeting NO, soluble guanylyl cyclase (sGC), cyclooxygenase, and the sympathetic and cholinergic pathways were used. Specifically, N(G)-nitro-L-arginine methyl ester (L-NAME, 100 µM), 1H-[1,2,4]oxadiazole[4,3-a]quinoxalin-1-one (ODQ, 30 µM), indomethacin (1 µM), propranolol (1 µM), and atropine (30 µM) were added 5–10 minutes prior to the administration of phenylephrine (PE, 1 µM).

In additional experiments, following confirmation of endothelial integrity, MF was added cumulatively at concentrations ranging from 10 to 320 µg/mL. In some preparations, the endothelium was mechanically removed by gently rubbing the intimal surface with a thread. The absence of endothelium was verified by the lack of vasorelaxation in response to acetylcholine (ACh, 1 µM). The contractile response to PE was used as a reference to normalize the effects of the test compound.

The effects of all obtained fractions and isolated compounds on aortic rings were evaluated; however, only those that exhibited vascular activity are presented.

Drugs

Phenylephrine hydrochloride, acetylcholine chloride, sodium nitroprusside, L-NAME, indomethacin, propranolol, and atropine were purchased from Sigma-Aldrich (Spain), while ODQ was obtained from the Cayman Chemical Company (Michigan, USA). Stock solutions were prepared in ultrapure water and stored at −20°C, except for indomethacin, which was dissolved in dimethyl sulfoxide (DMSO). Working dilutions were freshly prepared on the day of the experiments.

Statistical analysis

All data are presented as mean ± standard error of the mean (SEM). Differences in systolic blood pressure among SHR groups were assessed using two-way analysis of variance (ANOVA), followed by Bonferroni's post hoc test.

Vascular responses in aortic and mesenteric rings were expressed as a percentage of the initial contraction induced by PE. Dose-response curves for ACh and SNP were analyzed using nonlinear regression to determine the negative logarithm of the concentration required to produce 50% of the maximal effect (pEC_{50}).

Comparisons between concentration-response curves were performed using either the unpaired Student's t-test or the Mann–Whitney U test, depending on data distribution. Statistical significance was defined as $p<0.05$.

All statistical analyses were conducted using Microsoft® Excel 2013 and GraphPad Prism® version 6.

Regarding sample size, a total of 20 male SHRs were used and distributed into experimental groups of five animals each. Although no formal a priori power analysis was conducted, the group sizes were determined based on previously published studies employing comparable *in vivo* and *ex vivo* protocols and were deemed sufficient to detect biologically meaningful differences.

For the vascular reactivity experiments, an appropriate number of aortic and mesenteric rings were analyzed per treatment group. Sample sizes were selected based on the reproducibility and variability observed in prior organ bath studies and were sufficient to detect consistent pharmacological responses.

All statistical analyses were performed in accordance with the characteristics and distribution of the data. Detailed outputs, including summary statistics, *p*-values, and post hoc test results, are provided in the supplementary material (Figs. SM1–SM15, Tables SM1–SM2).

RESULTS

Structural elucidation of compounds isolated from *P. quadrangularis*

Compound **1** was isolated as a white powder and crystallized from MeOH:CH_2Cl_2; the molecular formula $C_{29}H_{48}O$ was deduced based on the HRMS spec-

trum, which displayed a pseudo-molecular ion peak at m/z 435,3602 [M+Na$^+$], which was supported by the ^{1}H and ^{13}C NMR spectral data.

The ^{1}H NMR spectra of compound **1** showed the presence of two methyl singlets at δ 0.69 (H-18) and 1.0 (H-19); a three-methyl doublet at δ 0.78 (H-26), 0.84 (H-27), and 1.02 (H-21); and a triplet at δ 0.81 (H-29). This compound also showed protons at δ 5.0 (H-23), 5.22 (H-22), and 5.33 (H-6), suggesting the presence of three protons corresponding to olefinic bonds and a proton at δ 3.51 (H-3) belonging to a sterol moiety.

The ^{13}C NMR values for all carbons are given in Table 1. The spectral data were supported by Heteronuclear Single Quantum Coherence (HSQC) correlations and are consistent with the reported literature values (Elgendy and Al-Ghamdy, 2007), allowing us to conclude that compound **1** corresponds to stigmasterol (Tables 1 and 2).

Compound **2** was isolated as a clear, oily liquid. The HRMS spectrum showed a pseudo-molecular ion peak at m/z 353.2680 [M+H$^+$], suggesting the molecular formula $C_{21}H_{36}O_4$. The ^{1}H NMR ($CDCl_3$) spectra contain methyl group signals at δ 0.96 (3H, t, *J*=7.5 Hz, H-18 linolenic). Methylene signals occur at δ 1.20-1.40 (8H, m, H-4, H-5, H-6, H-7), δ 1.50-1.60 (2H,m, H-3), δ 2.0-2.80 (4H, m, H-8, H-17), δ 2.34 (2H, t, *J* =7.3Hz, H-2), δ 2.80 (4H, m, H-11, H-14), δ 3.60 and 3.80 (2H, H-1′, H-3′), and δ 4.10-4.20 (2H, H-1′, H-3′). Methine signals are found at δ 3.90 (1H, m, H-2′) and δ 5.20-5.40 (6H, m, H-9, H-10, H-12, H-13, H-15, H-16, olefinic). The ^{13}C NMR ($CDCl_3$) values are δ: 14.4 (CH_3, C-18), 21.5 (CH_2, C-17), 23.6 (CH_2, C-14), 26.0 (CH_2, C-11), 26.4 (CH_2, C-8), 28.1 (CH_2, C-7), 30.2 (CH_2, C-6), 30.3 (CH_2, C-5), 21.5 (CH_2, C-4), 32.6 (CH_2, C-3), 34.9 (CH_2, C-2), 64.0 (C-1′), 64.5 (C-3′), 71.1 (C-2′), 128.2 (CH, C-9), 128.8 (CH, C-10), 129.2 (CH, C-12), 129.2 (CH, C-13), 131.0 (CH, C-16), 132.0 (CH, C-15), and 175.5 (CO, C-1). The comparison of NMR displacements with those found in the literature (Fraser et al., 2007; Guillén and Ruiz, 2003) allowed the identification of compound **2** as a long-chain unsaturated fatty acid ester of glycerol, corresponding to 2,3-dihydroxypropyl (9*Z*,12*Z*,15*Z*)-octadeca-9,12,15-trienoate (glyceryl linolenate); see Table 2 for its biological activities.

Compound **3** was isolated as a white, powdery substance. It was precipitated by changing the polarity (MeOH/ether) and the temperature. The HRMS spectrum showed a molecular formula of $C_{35}H_{58}O_6$ (m/z 597.4170 [M+Na$^+$]). Comparing the NMR values, the ^{13}C spectra reveal the presence of an anomeric carbon at δ 102.5 (C-1′) and oxygenated carbons in the sugar unit at δ 62.8-78.5 (C-2′, C-3′, C-4′, C-5′, and C-6′), as reported in the literature. These are close to those found in compound **1** with a glucose residue and, therefore, coincide with the steroidal saponin 3-*O*-*β*-D-glucopyranosyl stigmasterol (El-Askary, 2005) (Tables 1 and 2).

The extraction and isolation procedures for compounds **4** and **5** have been previously reported (Bareño et al., 2020). These compounds were identified as 3-*O*-*β*-D-glucopyranosyl oleanolic acid and 3-*O*-[*β*-D-glucopyranosyl–(1→2)-*β*-D-glucopyranosyl] oleanolic acid, respectively.

Both metabolites are considered key contributors to the vasoconstrictor effects observed in response to *P. quadrangularis* extract. The underlying mechanisms may involve the activation of voltage-dependent calcium channels and/or stimulation of α_2-adrenergic receptors.

Compound **6** was isolated as a yellow amorphous powder. The HRMS spectrum showed a molecular formula of $C_{26}H_{28}O_{14}$ (m/z 587.1387 [M+Na$^+$]). The ^{1}H NMR (MeOD) data showed two singlet protons at δ 6.57(1H, s, H-3) and 6.20 (1H, s, H-6) assigned to olefinic bonds on the A and C rings. There was also a four aromatic proton coupling system in the B ring at δ 7.95 (2H, d, *J*=8.8 Hz, H-2′, H-6′) and 6.92 (2H, d, *J* =8.8 Hz, H-3′, H-5′). The ^{13}C NMR and Distortionless Enhancement by Polarization Transfer (DEPT) spectra revealed the signals of 24 carbons, including one of carbonyl at δ 184.0 (C-4); oxygenated carbons at δ 162.8 (C-4′), 161.0 (C-5), 165.0 (C-7), 158.7(C-9) and 166.2 (C-2) assigned to a flavone aglycone; signals of sugar moieties between δ 62.9 and 82.7; and two anomeric carbons at δ 72.0 (C-1′′) and 106.2 (C-1′′′). Consequently, compound **6** was determined to be vitexin 2′′–*O*–xyloside (Tables 1 and 2) (Gil et al., 1998).

Compound **7** was isolated as a white solid. The HRMS spectrum showed a molecular formula of $C_{42}H_{70}O_{14}$ (m/z 821.4657 [M+Na$^+$]). The ^{13}C NMR (MeOD) data showed the presence of two anomeric carbons at δ 107. 0 (C-1′) and 102.4 (C-1′′); oxygenated carbons at δ 70.0 (C-1), 87.3 (C-3), 62.8 (C-21), and 67.9 (C-26); olefinic bond signals at δ 132.2 (C-25) and 132.2 (C-24); the signals of two hexoses at δ 60-85 ppm; and five methyl signals at δ 19.3 (C-18), 21.9 (C-27), 20.2 (C-28), 25.9 (C-29), and 15.3 (C-30). The ^{1}H NMR spectrum showed a pair of geminal cyclopropane protons at 0.40 (1H, s, H-19) and 1.01 (1H, s, H-19); the methylene signal at 24.4 (C-19) was affected by the oxygen bond of C-1 at 70.5. The HSQC spectrum revealed that the proton signal at δ 3.67 (1H, m, H-1) correlated with C-1.

The Heteronuclear Multiple Bond Correlation (HMBC) spectrum showed the correlation of the me-

thyl signals 0.91 (3H, s, H-29) and 0.84 (3H, s, H-30) with the oxygen bond at δ 87.2 (C-3); the anomeric carbon 107.0 (C-1′) with the singlet proton of H-3; quaternary carbons C-13 and C-14 with the signal protons of H-18 and H-28; the methine signal at δ 132.1 (C-24), and anomeric carbon 102.4 (C-1′′) with two protons of C-26. The signals found are similar to those presented by quadranguloside, a saponin first identified by Orsini et al. (1985), with a difference in the number of sugar units. Based on these findings, compound **7** was identified as 9,19-cyclolanost-24Z-ene-1*β*,3*β*,21,26-tetraol–3,26-di-*O*-*β*-D-glucoside, a cycloartanol-type triterpene saponin (see Tables 1 and 2). Notably, this compound has not been previously reported in *P. quadrangularis*.

Compound **8** was isolated as a white powder. The HRMS spectrum showed a pseudo-molecular ion peak at m/z 967.5239 [M+Na$^+$], suggesting the molecular formula $C_{48}H_{80}O_{18}$. The ^{1}H NMR (MeOD) spectrum showed four singlet methyl signals at δ 1.01 (3H, s, H-18), 0.93 (3H, s, H-28), 1.03 (3H, s, H-29) and 0.87 (3H, s, H-30); an olefinic methyl group at δ 1.77 (3H, s, H-27); a doublet proton signal characteristic of geminal cyclopropane protons at δ 0.33 (1H, d, *J* =4.2 Hz, H-19) and 0.57 (1H, d, *J* =4.2 Hz, H-19); and a double-bond olefinic proton between C-24 and C-25 at δ 5.41 (1H, s, H-24). The ^{13}C NMR (MeOD) data showed the presence of three anomeric carbons at δ 104.8 (C-1′), 108.6 (C-1′′), and 102.4 (C-1′′′). Three oxygenated carbon signals were identified in genins: the first corresponds to methine C-3 with a signal at 90.2, characteristic of glycosylated triterpenes in this position (Orsini et al., 1987); the other two correspond to methylenes at 62.7 (C-21) and 69.8 (C-26). The signals of three hexoses resonate at δ 60-85 ppm. The HMBC spectrum revealed that C-26 correlates with the anomeric carbon of C-1′′′ at δ 4.21 (1H, s, H-1′′′). The proton signals of the anomeric carbons 4.32 (1H, s, H-1′) and 4.33 (1H, m, H-1′′) correlated with the anomeric carbon 104.8 (C-1′); this, in turn, correlated with the signal 90.2 (C-3); the signal 67.9 (C-6′) correlated with the proton of the anomeric carbon of C-1′′, indicating a 1→6 union between these two sugars, and the anomeric protons resonates in a range between δ_H 4.2-4.8 ppm, suggesting a *β* configuration in each of the monosaccharide units. The structure of compound **8** was proposed by Orsini et al. (1987), but it was isolated as a mixture. It is very similar to that of quadranguloside identified by Orsini et al. in 1985 in *P. quadrangularis* and by Reginatto et al. (2001) in *P. alata*, with the difference of a hexose linked through the sugar unit present in C-26. Based on the above and Reginatto et al.'s results, it was possible to establish that compound **8** is 9,19-cyclolanost-24Z-ene-3*β*,21,26*β*-triol-3-*O*-*β*-D-gentibioside-26-*O*-*β*-D-glucopyranoside (Tables 1 and 2).

Table 1. ^{1}H and ^{13}C (400 MHz) chemical shifts of compounds 1,3,7,8 and 6.

	1		**3**		**7**		**8**			**6**	
	($CDCl_3$)		**(Pyr-d_5)**		**(MeOD)**		**(MeOD)**			**(MeOD)**	
	(Elgendy and Al-Ghamdy, 2007)		**(El-Askary, 2005)**		**(Reginatto et al.,2001)**		**(Reginatto et al., 2001)**			**(Ferreres et al., 2007)**	
Carbon	**^{1}H (δ)**	**^{13}C(δ)**	**^{1}H (δ)**	**^{13}C(δ)**	**^{1}H (δ)**	**^{13}C(δ)**	**^{1}H (δ)**	**^{13}C(δ)**	**Carbon**	**^{1}H (δ)**	**^{13}C(δ)**
1	1.80 m	37.2	1.72 m	37.4	3.67 s	70.5		32.1	**2**		166.2
2		31.5		29.3		41.4		31.0	**3**	6.57 s	103.4
3	3.51 m	71.1		78.0	3.30 m	87.2	3.27 m	90.2	**4**		184.0
4	2.30 m	42.2		39.3		41.4		42.0	**5**		161.0
5		140.8	5.36 m	140.9		47.5		48.6	**6**	6.20 s	99.6
6	5.33 m	121.6	5.34 m	121.9		22.8		22.1	**7**		165.0
7	1.50-1.70 m	31.5		32.1		28.4		27.6	**8**		104.0
8	1.50-1.70 m	31.8		32.0		51.9		49.0	**9**		158.7
9		50.1	1.55 m	50.3		22.6		21.1	**10**		105.1
10		36.4		36.9		32.1		27.0	**1'**		121.0
11		21.0		21.3		25.2		27.5	**2'**	7.95 d *J*=8.8 Hz	130.0

Table 1. ^{1}H and ^{13}C (400 MHz) chemical shifts of compounds 1,3,7,8 and 6 (continued...)

	1		**3**		**7**		**8**			**6**	
	($CDCl_3$)		**(Pyr-d_5)**		**(MeOD)**		**(MeOD)**			**(MeOD)**	
	(Elgendy and Al-Ghamdy, 2007)		**(El-Askary, 2005)**		**(Reginatto et al.,2001)**		**(Reginatto et al., 2001)**			**(Ferreres et al., 2007)**	
Carbon	**^{1}H (δ)**	**^{13}C(δ)**	**^{1}H (δ)**	**^{13}C(δ)**	**^{1}H (δ)**	**^{13}C(δ)**	**^{1}H (δ)**	**^{13}C(δ)**	**Carbon**	**^{1}H (δ)**	**^{13}C(δ)**
12	2.0 m	3.6		39. 8		37.8	1.34 s	36.7	**3'**	6.92 d *J*=8.8 Hz	117.1
13		42.2		42.3		45.9		46.4	**4'**		162.8
14		56.8		56.9		50.2		48.8	**5'**	6.92 d *J*=8.8 Hz	117.1
15		24.3		24.5		33.7		33.2	**6'**	7.95 d *J*=8.8 Hz	130.0
16		28.9		29.3		31.0	2.03 s	27.3	**1''**	5.03 d *J*=10.0 Hz	71.0
17		55.9		56.1		44.0	1.54 s	43.5	**2''**	4.30 d *J*=9.0 Hz	80.9
18	0.69 s	19.7	0.66 s	12.1	0.96 s	19.3	1.01 s	19.2	**3''**	3.0-3.50 m	77.3
19	1.0 s	21.1	0.91 s	19.4	1.01 s	24.4	0.33 d *J*= 4.2Hz	31.0	**4''**	3.0-3.50 m	70.9
					0.40 s		0.57 d *J*= 4.2Hz		**5''**	3.66 m	82.7
20		40.4		40.7		46.2		47.4	**6''**	3.80 m	62.9
21	1.02 d *J*= 7.0 Hz	12.0		21.4	3.69 m 3.84 m	62.8		62.7	**1'''**	4.14 d *J*=7.3 Hz	106.2
22	5.0 dd *J*=8.6 J=15.0 Hz	129.2	5.20 dd *J*= 8.7 *J*=15.0 Hz	138.8		31.0		30.7	**2'''**	2.96 t *J*=8.0 Hz	73.7
23	5.22 dd *J*=8.6 *J*= 15.0 Hz	183.3	5.06 m	129.4		27.2		25.3	**3'''**	2.97 m	75.1
24		51.2		51.4	5.40 s	132.2	5.41 s	132.1	**4'''**	3.92 m	70.8
25		31.8		32.0		132.1		132.3	**5'''**	2.60 t *J*=12.0 Hz	66.6
26	0.78 d *J*=6.9 Hz	18.3		21.3	4.33 d *J*=8.0 Hz 4.22 d *J*=8.0 Hz	67.9	4.38 s 4.21 s	67.9		3.0 m	
27	0.84 d *J*=6.9 Hz	18.9		19.2	1.75 s	21.9	1.77 s	22.0			
28		25.3		25.7	0.93 s	20.2	0.93 s	20.1			
29	0.81 t *J*=7.0 Hz	11.7		12.5	0.91 s	25.9	1.03 s	26.0			
30					0.84 s	15.3	0.87 s	15.9			
1'			5.06 m	102.5	4.31 d *J*=8.0 Hz	107.0	4.32 s	104.8			
2'			4.06 t *J*=8.0 Hz	75.3	3.20 m	75.0	3.18-3.33 m	75.0			
3'			4.30 m	78.5	3.30 m	77.9	3.18-3.33 m	78.1			
4'			4.30 m	71.6	3.31 m	72.0	3.18-3.33 m	71.4			
5'			3.96 m	78.4	3.18 m	75.6	3.18-3.33 m	75.6			

Table 1. ^{1}H and ^{13}C (400 MHz) chemical shifts of compounds 1,3,7,8 and 6 (continued...)

	1		**3**		**7**		**8**			**6**	
	($CDCl_3$)		**($Pyr\text{-}d_5$)**		**(MeOD)**		**(MeOD)**			**(MeOD)**	
	(Elgendy and Al-Ghamdy, 2007)		**(El-Askary, 2005)**		**(Reginatto et al.,2001)**		**(Reginatto et al., 2001)**			**(Ferreres et al., 2007)**	
Carbon	**^{1}H (δ)**	**^{13}C(δ)**	**^{1}H (δ)**	**^{13}C(δ)**	**^{1}H (δ)**	**^{13}C(δ)**	**^{1}H (δ)**	**^{13}C(δ)**	**Carbon**	**^{1}H (δ)**	**^{13}C(δ)**
6'			4.2 dd *J*=5.2 *J*=11.7 Hz	62.8	3.83 m	62.8	4.10 d *J*=12.7	69.8			
			4.55 dd J=2.2 *J*=11.7 Hz				3.80 m				
1''					4.23 d *J*=8.0 Hz	102.4	4.33 m	108.6			
2''					3.20 m	75.1	3.18-3.33 m	75.0			
3''					3.33 m	78.1	3.18-3.33 m	78.3			
4''					3.30 m	71.9	3.18-3.33 m	71.5			
5''					3.33 m	77.7	3.18-3.33 m	77.7			
6''					3.65 m	62.8		62.8			
1'''							4.21 s	102.4			
2'''							3.18-3.33 m	75.1			
3'''							3.18-3.33 m	77.9			
4'''							3.18-3.33 m	71.6			
5'''							3.18-3.33 m	77.0			
6'''								62.8			

Table 2. Compounds obtained of CH_2Cl_2 fraction of *P. quadrangularis* L. and their pharmacological activities.

Compound name	**Chemical structure**	**Pharmacological activities**	**References**
Stigmasterol	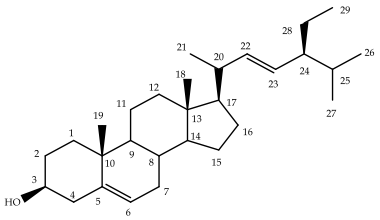	Anticancer, anti-osteoarthritis, anti-inflammatory, anti-diabetic, immunomodulatory, antiparasitic, antifungal, antibacterial, antioxidant, and neuroprotective properties.	Bakrim et al., 2022; Pratiwi et al., 2021
2,3-Dihydroxypropyl (9*Z*,12*Z*,15*Z*)-octadeca-9,12,15-trienoate (glyceryl linolenate)	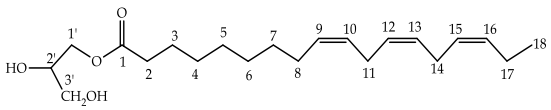	Anti-inflammatory, antithrombotic, antiarrhythmic, and vasodilator, hyperlipidemia, hypertension, depression and rheumatoid arthritis.	Shahidi and Finley, 2001; Kapoor and Patil, 2011
3-*O*-*β*-D-Glucopyranosyl stigmasterol	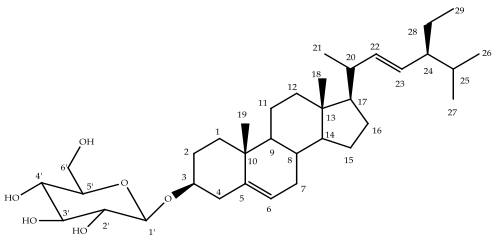	Anti-inflammatory, antioxidant, and neuroprotective properties.	Amina et al., 2018; Bakrim et al., 2022; Khabazian et al., 2002; Pratiwi et al., 2021

Table 2. Compounds obtained of CH_2Cl_2 fraction of *P. quadrangularis* L. and their pharmacological activities (continued...)

Compound name	Chemical structure	Pharmacological activities	References
3-*O*-*β*-D-Glucopyranosyl oleanolic acid	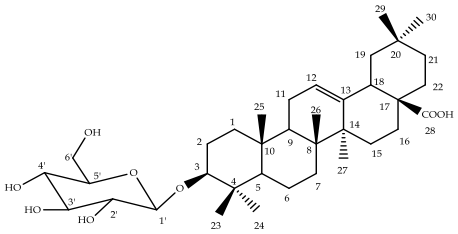	Anti-inflammatory, antioxidant, hepatoprotective, anticancer, neuroprotective, anti-diabetic, anti-hyperlipidemic, nephroprotective, anti-osteoporotic effects, anti-hypertensive and cardiovascular protection.	Ayeleso et al., 2017; Pollier and Goossens, 2012; Sen, 2020
3-*O*-[*β*-D-Glucopyranosyl– (1→2)-*β*-D- glucopyranosyl] oleanolic acid	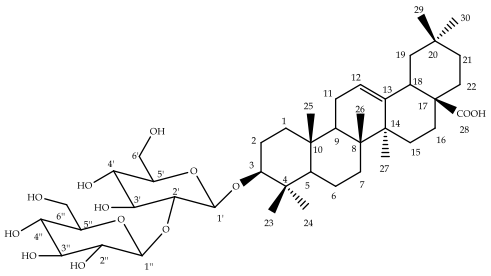	Anti-inflammatory, antioxidant, hepatoprotective, anticancer, neuroprotective, anti-diabetic, anti-hyperlipidemic, nephroprotective, anti-osteoporotic effects, anti-hypertensive and cardiovascular protection.	Ayeleso et al., 2017; Pollier and Goossens, 2012; Sen, 2020
Vitexin 2''-*O*–xiloside	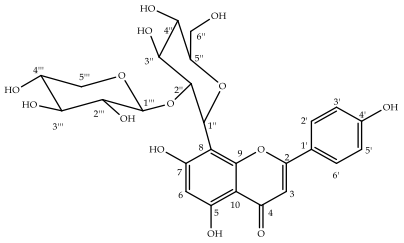	Cardiovascular protection, anti-cancer, antioxidant, anti-inflammatory, anti-nociceptive, anti—Alzheimer disease (AD), neuroprotective, anti-hypertensive, anti-spasmodic, anti-hypoxia/ischemia injury, anti-depressant-like actions and anti-viral activities.	Che et al., 2016; He et al., 2016
9,19-Cyclolanost-24Z-ene-1*β*,3*β*,21,26-tetraol–3,26-di-*O*-*β*-D-glucoside	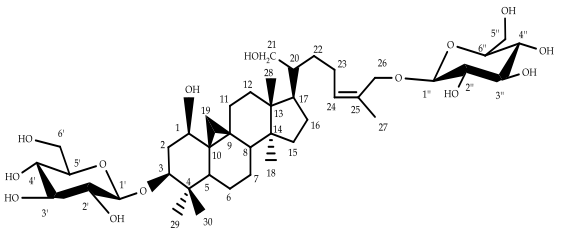	This compound is reported for the first time for *Passiflora quadrangularis* L. In general, the cycloartane triterpenoid saponins compounds have shown antidepressant, anti-inflammatory and anti-hypertensive, anti-cancer effects.	Lee et al., 2013; Man et al., 2010; Wang et al., 2013
9,19-Cyclolanost-24Z-ene-3*β*,21,26*β*-triol3-*O*-*β*-gentibioside-26-*O*-*β*-D-glucopyranoside	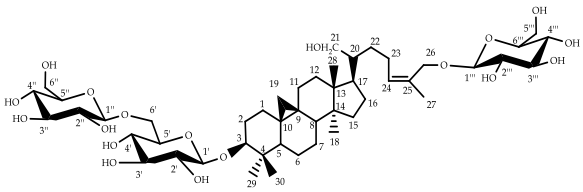	The cycloartane triterpenoid saponins compounds have shown antidepressant, anti-inflammatory and anti-hypertensive, anti-cancer effects	Lee et al., 2013; Man et al., 2010; Wang et al., 2013
γ-Aminobutyric acid (GABA)	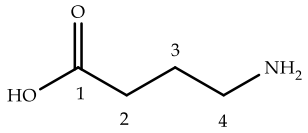	Neurological disorder prevention, neuroprotective, anti-diabetic, anti-inflammatory, anti-microbial, anti-allergic, hepatoprotective, reno protective, anti-hypertensive, anti-cancer, and antioxidant effects.	Ngo and Vo, 2019
β-Carbolinic alkaloids	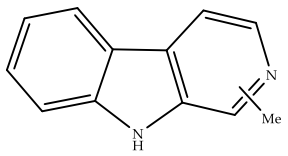	Anti-inflammatory, antithrombotic, anti-cancer, anti-virus, anti-bacterial, anti-spasmodic, emetic, astringent, anti-Parkinson activities; treatment hypertension, myocardial infarction, and atherosclerosis	Moloudizargari et al., 2013; Zhang et al., 2021

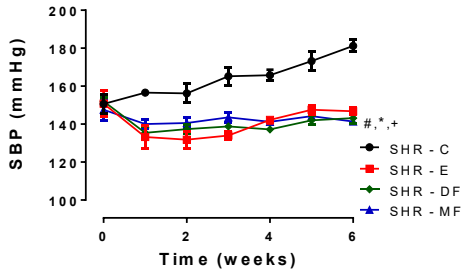

Figure 2. Effect in systolic blood pressure (SBP) on spontaneously hypertensive rats (SHRs) by administration of 75 mg/kg/day of E#, DF*, and MF+.

Data are mean values ± SEM for 5 rats. #,*,+p<0.05 versus C. C: control; E: Total extract of *P. quadrangularis*; DF: CH_2Cl_2 fraction; MF: MeOH fraction.

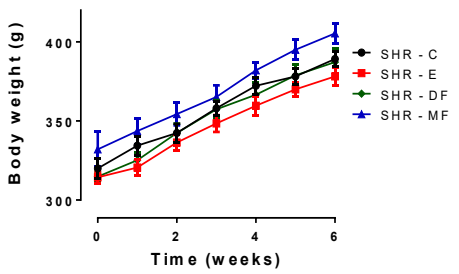

Figure 3. Body weight on spontaneously hypertensive rats (SHRs) by administration of 75 mg/kg/day of E, DF, MF, and C.

Data are mean values ± SEM for 5 rats. C: control; E: Total extract of *P. quadrangularis*; DF: CH_2Cl_2 fraction; MF: MeOH fraction.

Compound **9** was isolated as a viscous brown liquid. The HRMS spectrum showed the molecular formula of $C_4H_9NO_2$ (m/z 126.0535 [M+Na$^+$]). The ^{1}H and ^{13}C NMR spectrum revealed two methylene signals at δ 36.5 (C-2), 2.29 (2H, t, *J* =7 Hz, H-2) and 25.6 (C-3),1.83 (2H, t, *J* =7 Hz, H-3), a carbonyl group signal at δ 181.1 (C-1), and a methylene amino group at δ 41.1 (C-4), δ_H 2.92 (2H, t, *J*=7 Hz, H-4). The above suggests that compound **9** is γ-aminobutyric acid (GABA) (Table 2) (Zahmanov et al., 2015).

Through the spectral analysis of the dicloromethane fraction (**DF-8**) we were able to identify some signals of *β*-carboline alkaloids, such as ^{1}H NMR (400 MHz, CD_3OD) δ: 2.29 (1H, m, N-2H) and 9.40 (1H, s, N-9H) corresponding to its amino groups. The signals of proton attached to C-4 [δ: 3.22 (1H, d, H-4), 3.40 (1H, d, H-4), and 4.23 (1H, q, H-3)] and to aromatic structures (δ: 6.05-6.20 (1H, m, H-5, 6, 7,8)) (Table 2) (Zeng et al., 2010).

Antihypertensive effect of *P. quadrangularis* fractions and extract

In a preliminary study using Wistar rats, the extract of *P. quadrangularis* was found to prevent L-NAME-induced hypertension, enhance endothelium-dependent vasodilation, and protect against vascular remodeling at all tested doses (75, 150, and 300 mg/kg body weight) (Bareño et al., 2017).

Based on these findings, a dose of 75 mg/kg body weight of the extract, DF, and MF were selected for further evaluation in SHRs. SBP was measured following administration.

The mean SBP at baseline (week 0) was 150 ± 1 mmHg, with no significant differences between treatment groups. From week 1 onward, all treated groups exhibited significantly lower SBP values compared to the control group. This effect was supported by a two-way ANOVA, which showed a statistically significant interaction between treatment and time ($F_{(18,11)} = 3.45$, $p<0.0001$), a significant main effect of treatment ($F_{(3,11)} = 76.02$, $p<0.0001$), and of time ($F_{(6,11)} = 7.66$, $p<0.0001$). Bonferroni's post hoc test confirmed significant differences between the treated groups and the control group from week 1 to week 6 ($p<0.05$). No significant differences were observed between the E, DF, and MF groups (Fig. 2, Fig. SM1). Body weight increased progressively across all groups throughout the experimental period (Fig. 3).

Vascular responses

SHR experiments

The α_1-adrenergic agonist PE, used as a preconstrictor, was applied at a concentration of 0.1 µM in aortic rings and 3 µM in mesenteric rings. In aortic rings, PE induced a maximal contractile response of 1076 ± 86 mg in the control group (C), 1181 ± 64 mg in E, 874 ± 52 mg in DF, and 1174 ± 74 mg in MF (Fig. SM2). In mesenteric rings, the contractile responses were 2.17 ± 0.29 mN in C, 2.53 ± 0.26 mN in E, 2.83 ± 0.56 mN in DF, and 2.92 ± 0.38 mN in MF (Fig. SM4). One-way ANOVA followed by Dunnett's multiple comparisons test revealed no statistically significant differences between any treatment group and the control in either vascular bed ($p>0.05$ for all comparisons; Figs. SM3 and SM5). These findings indicate that PE-induced pre-constriction was comparable across groups, ensuring consistent baseline tone prior to the evaluation of vasodilator responses.

Aortic and mesenteric rings from treated rats showed greater ACh-induced relaxation than arteries from the control group, indicating improved endothelial function. The concentration–response curves of all treatments shifted to the left, favoring the EC_{50}. One-way ANOVA revealed significant differences in the E, DF, and MF groups compared to the control ($F = 63.04$, $p<0.0001$; Bonferroni post-test). Similarly, in mesenteric rings, all treatments (E, DF, and MF)

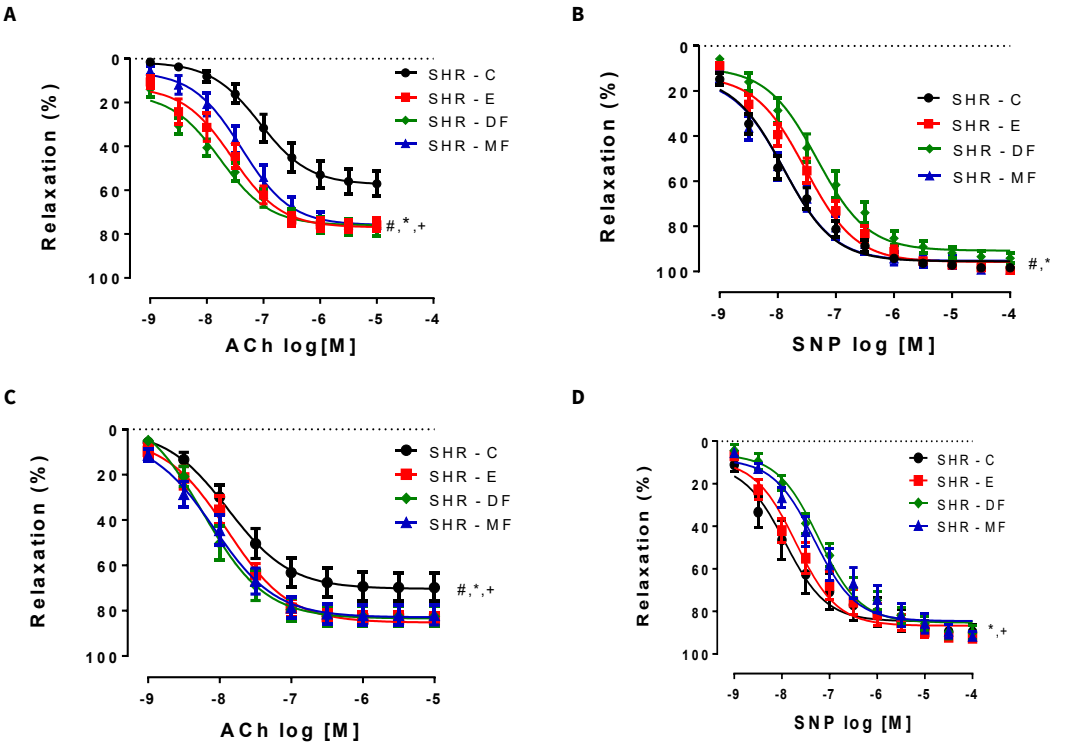

Figure 4. Cumulative concentration-response curves to (**A**) Ach, (**B**) sodium nitroprusside (SNP) in pre-constricted aorta rings; cumulative concentration-response curves to (**C**) acetylcholine (ACh) and (**D**) SNP in pre-constricted mesenteric rings from spontaneously hypertensive rats (SHRs) by administration of 75 mg/kg/day of E#, DF* and MF+.

Data are mean values ± SEM for 5 rats $^{\#,*,+}p<0.05$ versus C. C: control; E: Total extract of *P. quadrangularis*; DF: CH_2Cl_2 fraction; MF: MeOH fraction.

produced significant differences compared to the control (F = 31.70, p<0.0001; Bonferroni post-hoc test) (Fig. 4, Table SM1, Figs. SM6 and SM7).

As shown in Fig. 4, SNP-induced relaxation was observed in both aortic and mesenteric rings. In aortic rings, treatments with E and DF showed significant differences in potency compared with C, with mean differences of 5.29 (95% CI: 0.72 to 9.86, p=0.03) and 12.80 (95% CI: 6.16 to 19.44, p<0.001), respectively. No significant differences were observed between the C and the MF (mean difference = 0.075, p>0.99). The ANOVA for the aorta data was significant (F = 26.02, p<0.001), confirming overall treatment effect (Fig. SM8).

In mesenteric rings, the DF and MF fractions also showed statistically significant differences in potency compared with the C, with mean differences of 10.56 (95% CI: 1.60 to 19.50, p=0.02) and 8.91 (95% CI: 1.71 to 16.11, p=0.02), respectively. E fraction did not differ significantly from C (mean difference = 1.96, p>0.99). The corresponding ANOVA also indicated a significant treatment effect in mesenteric rings (F = 12.95, p=0.003) (Fig. SM9).

In PE-stimulated aortic rings, statistically significant differences were observed only in the groups treated with the DF and MF fractions when compared to the control (Table SM1).

Wistar rat experiments

As previously reported, the ethanolic extract of *P. quadrangularis* exhibits a notable antihypertensive effect *in vivo*. However, *in vitro* experiments have shown a paradoxical vasoconstrictor effect (Bareño et al., 2020).

A similar response was observed with the MF, which induced concentration-dependent contractions in both endothelium-intact and endothelium-denuded aortic rings, with no significant differences between the two conditions (p>0.47). The maximal contractile response (E_{max}) and potency (pEC_{50}) were as follows: intact rings, E_{max} = 105 ± 3%, pEC_{50} = 4.0 ± 0.0; denuded rings, E_{max} = 90 ± 2%, pEC_{50} = 4.1 ± 0.0 (Fig. 5).

The DF exhibited a tendency to induce smooth muscle relaxation; however, this effect appeared to be partially masked by a superimposed contractile response (data not shown). This contractile component is likely attributable to the presence of oleanolic acid-derived saponins (compounds **4** and **5**), whose vasoconstrictor activity has been previously reported (Bareño et al., 2020).

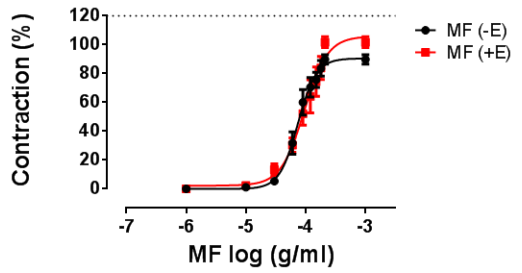

Figure 5. Cumulative concentration-response curves to MeOH fraction (MF) in endothelium intact (E+) and denuded (E-) the aortic rings of Wistar rats.

Data are mean values ± SEM for 6 rings per treatment. p>0.05.

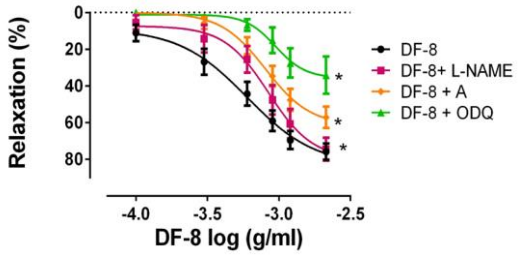

Figure 6. Cumulative concentration-response curves to dichloromethane subfraction DF-8 in aorta rings from Wistar rats, previously addition of L-NAME (100 µM), 1H-[1,2,4]oxadiazole[4,3-a]quinoxalin-1-one (ODQ, 30 µM), and atropine (30 µM).

Data are mean values ± SEM for 6 rings per treatment. *p<0.05 versus DF-8.

The dichloromethane subfraction DF-8 induced vasodilation in precontracted aortic rings, with a maximal relaxation response (E_{max}) of 83 ± 5%. This effect was significantly attenuated in the presence of L-NAME, atropine, and ODQ (Table 3, Fig. 6).

Table 3. E_{max} and pEC_{50} of DF-8 in aortic rings of Wistar rats with L-NAME, indomethacin, propranolol.

Antagonist	DF-8	
	E_{max} (%)	pEC_{50}
C	83 ± 4.69	3.22 ± 0.03
L-NAME (100 µM)	80 ± 4.87*	3.07 ± 0.02*
Indomethacin (1 µM)	80 ± 3.41	3.21 ± 0.02
Propranolol (1 µM)	77 ± 3.55	3.15 ± 0.03
Atropine (30 µM)	61 ± 3.76*	3.09 ± 0.02*
ODQ (30 µM)	36 ± 3.61*	3.02 ± 0.03*

The results are expressed as mean ± SEM of the number of dates of 6 rings per treatment. pCE_{50}(-logCE_{50}, g/mL) and E_{max} (percent of 1 µM, PE maximal contraction). Units for CE_{50} are expressed as M *p<0.05 vs. C: Control; ODQ: 1H-[1,2,4]oxadiazole[4,3-a]quinoxalin-1-one.

Statistical analysis confirmed significant differences in the relaxation response when rings were pretreated with L-NAME (p=0.01), atropine (p<0.001), or ODQ (p<0.01), whereas no significant changes were observed with propranolol (p=0.12) or indomethacin (p=0.44) (Table 3).

These findings suggest that the vasodilatory effect of DF-8 is mediated, at least in part, by the NO–cGMP signaling pathway and muscarinic receptor activation.

Vitexin 2''–*O*–xyloside (compound **6**) induced concentration-dependent vasodilatation, with a maximal relaxation response (E_{max}) of 12 ± 1%. This effect was attenuated in the presence of L-NAME (p<0.001) and ODQ (p<0.01) (data not shown), suggesting involvement of the NO–cGMP signaling pathway. These findings are consistent with previous reports describing the vasorelaxant properties of vitexin derivatives, which are mediated through endothelial NO production (Ameen and Al-Habib, 2021).

Cardiac and aortic hypertrophy and fibrosis

Among all the treatment groups, only the DF fraction produced a statistically significant reduction in the left ventricular wall thickness-to-heart radius ratio (W_{LV}/R) compared to the control (C = 0.74 ± 0.03; DF = 0.57 ± 0.30; p<0.05). This was confirmed by the Kruskal-Wallis test followed by Dunn's post hoc analysis. No significant differences were found in the remaining groups or in other morphometric parameters, including those related to the aorta (Table SM2, Fig. SM13).

Nevertheless, significant reductions in both cardiac and aortic fibrosis were observed in all treatment groups compared to control, as assessed in histological sections stained with Sirius Red and Masson's Trichrome, respectively (Figs. 7 and 8). For cardiac fibrosis, the Kruskal-Wallis test indicated a statistically significant difference among groups (p<0.0001), and Dunn's post hoc analysis confirmed reductions in fibrosis for all treatments (C vs. E: ****, C vs. DF: ****, C vs. MF: ***). Regarding aortic fibrosis, one-way ANOVA also showed a significant treatment effect ($F(3, 56) = 14.58$, p<0.0001), and Bonferroni's multiple comparisons test revealed significant differences between the control and all treatment groups (C vs. E: **, C vs. DF: ****, C vs. MF: ****).

DISCUSSION

Previous phytochemical studies have identified key secondary metabolites in *P. quadrangularis*, including flavonoids, β-carboline alkaloids (such as harmane), and both steroidal and triterpene saponins (Bareño et al., 2017; Costa et al., 2013; Ingale and Hivrale, 2010; Orsini et al., 1985; 1987; Sakalem et al., 2011).

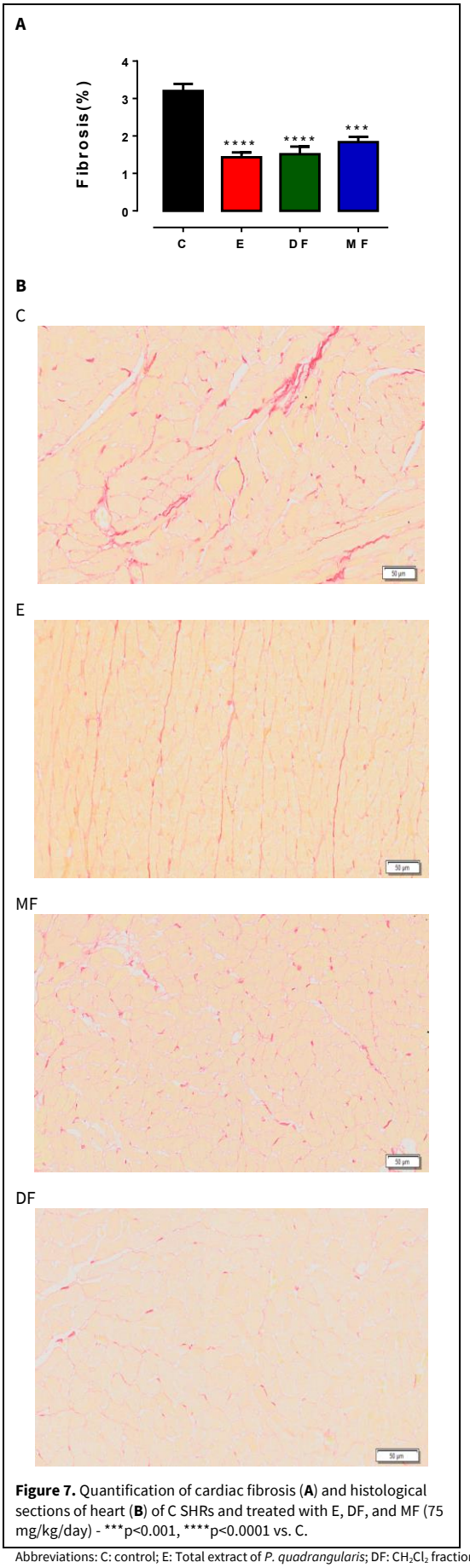

Figure 7. Quantification of cardiac fibrosis (**A**) and histological sections of heart (**B**) of C SHRs and treated with E, DF, and MF (75 mg/kg/day) - ***p<0.001, ****p<0.0001 vs. C.

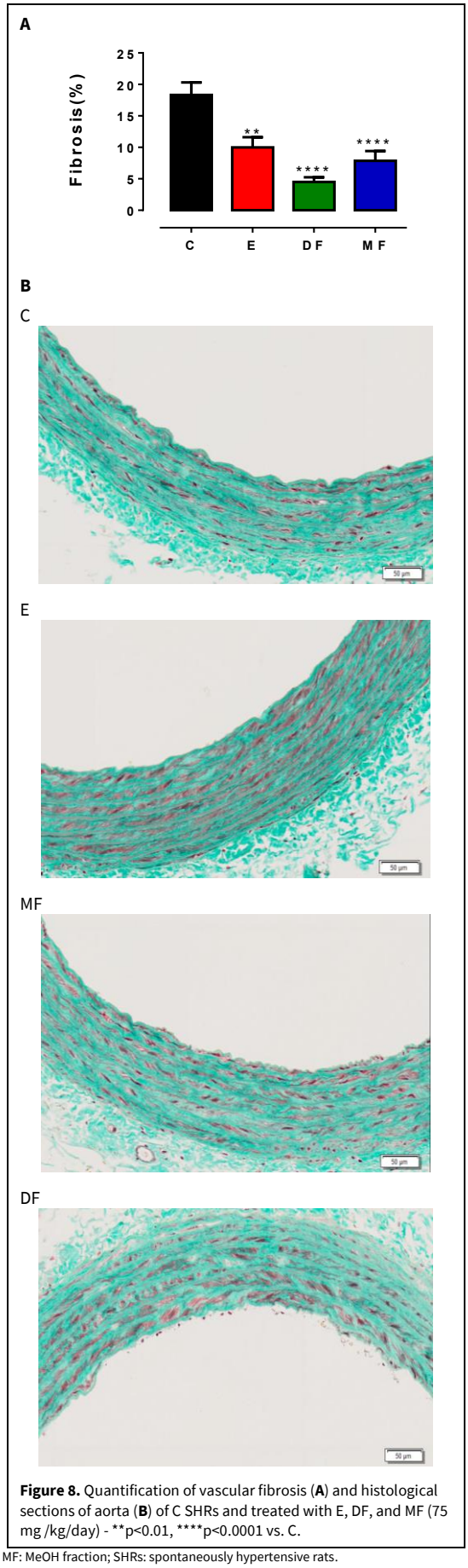

Figure 8. Quantification of vascular fibrosis (**A**) and histological sections of aorta (**B**) of C SHRs and treated with E, DF, and MF (75 mg /kg/day) - **p<0.01, ****p<0.0001 vs. C.

Abbreviations: C: control; E: Total extract of *P. quadrangularis*; DF: CH_2Cl_2 fraction; MF: MeOH fraction; SHRs: spontaneously hypertensive rats.

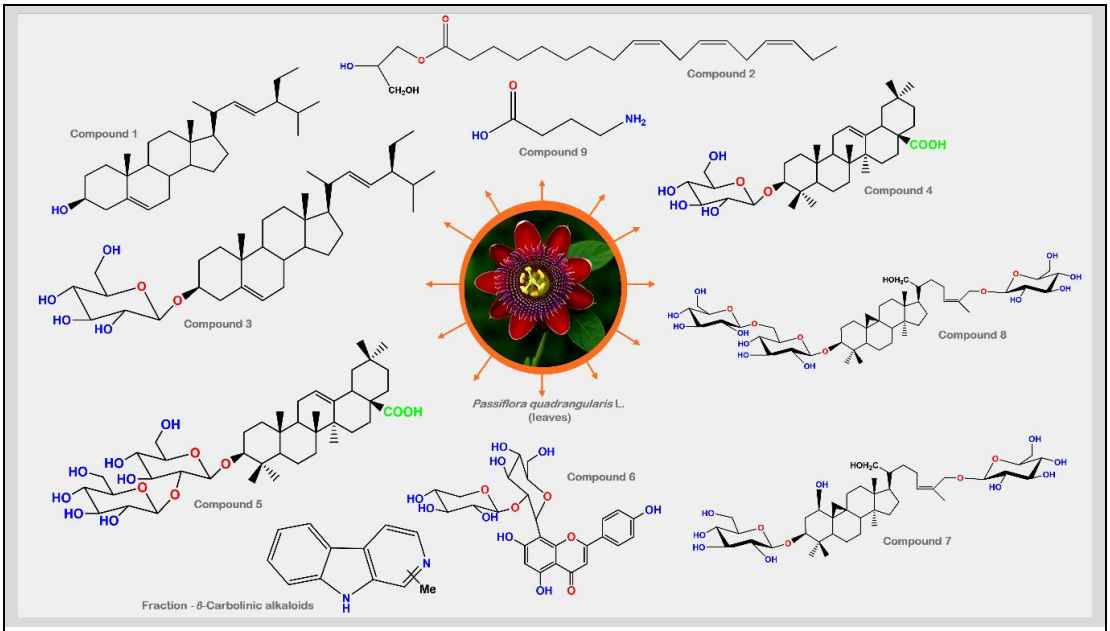

Figure 9. Chemical structures of compounds isolated and identified from the leaves of *Passiflora quadrangularis* L.

In the present study, fractionation of the total extract enabled the structural elucidation of nine compounds. Among these, compounds **7** and **9** are reported here for the first time in *P. quadrangularis*. Notably, compound **8** had been previously proposed by Orsini et al. (1987), but its structure could not be confirmed at that time due to its isolation as part of a mixture. Our findings now provide structural confirmation of this compound in its pure form (Fig. 9).

All isolated fractions and compounds were evaluated using *in vitro* assays; however, only those exhibiting vascular activity are presented in this study.

The evaluated DF and MF fractions contain similar classes of compounds in varying proportions, including vitexin-type flavonoids, β-carboline alkaloids (e.g., harmane), triterpene saponins derived from oleanolic acid, and cycloartanol-type triterpenoids. Notably, the DF fraction contains β-carboline alkaloids, which are absent in the MF fraction. Conversely, the MF fraction has a higher content of triterpenes compared to DF.

These compositional differences likely contributed to the distinct vascular responses observed in aortic and mesenteric rings from spontaneously SHRs (Fig. 4; Table SM1), as well as in the aortic rings of Wistar rats (Figs. 5 and 6; Table 3).

However, given the variability of compounds present in the fractions, and although many of these metabolites have documented cardiovascular effects, it is not possible to assign the observed activity to a specific compound. Additionally, possible interactions among the constituents, whether synergistic, additive, or antagonistic, may contribute to the overall vascular effects.

The findings indicate that the oral administration of the DF, MF, and extract of *P. quadrangularis* at 75 mg/kg body weight per day significantly reduced SBP by 40 mmHg compared to the control group, starting from the first week of treatment.

All treatments attenuated the progression of hypertension, improved endothelium-dependent relaxation, and decreased cardiac hypertrophy (Fig. 7) and vascular remodeling (Fig. 8). Notably, the magnitude of SBP reduction observed with these treatments was comparable to that reported for conventional antihypertensive agents such as captopril and verapamil (Al-Akwaa et al., 2020; Song et al., 2021; Zhang et al., 2023).

Previous studies have shown that the extract and fractions of *P. quadrangularis* can prevent cardiac hypertrophy and vascular remodeling in rats subjected to NO deficiency (Bareño et al., 2017).

In the present study, histopathological analysis of heart and aortic tissue sections revealed that the control group exhibited increased interstitial collagen deposition and structural alterations in vascular and myocardial cells compared to the treatment groups (Figs. 7 and 8).

Some studies have suggested that 19-month-old SHRs exhibit a higher hypertrophy index than 4 to 11-month-old animals (Álvarez et al., 2008), highlighting the progressive nature of cardiac remodeling with age. In our study, histopathological sections of the heart and aorta showed that the control group exhibited increased interstitial collagen and structural

changes in cells compared with the treatment groups (Figs. 7 and 8).

Cardiac and aortic collagen accumulation was prevented by *P. quadrangularis* extract and fractions. Although morphometric studies only demonstrated significant differences in the W_{LV}/R parameter for the DF fraction, its tendency to prevent remodeling is evident (Table SM2). We found that the E, DF, and MF treatments effectively controlled remodeling factors like cardiomyocyte size and the extracellular matrix and attenuated collagen accumulation compared to the control group. Nevertheless, considering the progressive hypertrophy described in aged SHRs, longer treatment periods and longitudinal evaluations would be necessary to confirm the persistence and stability of these effects over time.

Oxidative stress is a deleterious process that can damage cell structures and may be responsible for persistent elevated SBP, increased cardiac hypertrophy, or both.

Vitexin (compound **6**) exhibits potent free radical scavenging activity and shows a protective effect against H_2O_2-induced oxidative damage, as reported in previous studies. It also has a cardioprotective effect, related to inhibiting the release of inflammatory cytokines and myocardial apoptosis (Che et al., 2016).

Its antihypertensive effects have been associated with mechanisms involving K^+ channels, cGMP, PGI_2, and the nitric oxide synthase (NOS) pathway (Ameen and Al-Habib, 2021; Mali et al., 2012). In the present study, vitexin was evaluated in isolated aortic rings precontracted with phenylephrine, and its vasodilatory effect appeared to be attenuated in the presence of the NOS inhibitor L-NAME and the soluble guanylate cyclase inhibitor ODQ (data not shown), supporting the involvement of the NO/cGMP signaling pathway. However, further molecular studies are required to fully elucidate these mechanisms and confirm the specific contribution of vitexin within the complex extract.

Furthermore, the FD-8 fraction, primarily composed of β-carboline alkaloids, exhibited vasorelaxant effects in assays using isolated rat thoracic aorta rings (Fig. 6). This vasorelaxant response was attenuated in the presence of NOS and cyclic GMP (cGMP) inhibitors, as well as by the activation of cholinergic receptors. These findings are consistent with previous reports and support the hypothesis that β-carboline alkaloids may possess antioxidant properties and exert protective effects on cardiomyocytes (Moloudizargari et al., 2013; Shi et al., 2000).

Based on the aforementioned findings, activation of the NO pathway may stimulate Na+/K^+-ATPase activity and promote the opening of K^+ channels, potentially contributing to the regulation of vascular tone in resistance arteries. Additionally, NO induces cGMP production by activating guanylyl cyclases (GCs), a hyperpolarizing factor that increases K^+ channel permeability (Fiorim et al., 2012). Endothelium-derived hyperpolarizing factor (EDHF) plays a role in maintaining normal vascular tone and mediates greater relaxation in resistance vessels compared to conductance vessels. The K^+ channel itself has been proposed to act as an EDHF (Rameshrad et al., 2016). However, these proposed mechanisms are based on *in vitro* data, and further molecular studies are necessary to confirm the precise pathways involved in the vasorelaxant effect of the FD-8 fraction.

The cumulative concentration–response curves of DF, MF, and E to ACh, together with the histological sections, suggest improved endothelium-dependent relaxation in both aortic and mesenteric rings. This enhanced vasorelaxation could be associated with increased NO bioavailability and subsequent endothelial protection. The improved endothelial function may contribute to reduced fibrosis, a factor commonly involved in cardiac remodeling. Additionally, elevated intracellular cGMP levels are known to exert cytoprotective effects against nitro-oxidative stress (Korkmaz et al., 2013). Moreover, activation of endothelial M_3 muscarinic receptors, known to mediate ACh-induced vasodilation, could contribute to the observed vascular relaxation in the mesenteric bed (Tangsucharit et al., 2016).

The vasoconstrictor effect of the MF fraction was not affected by the absence of endothelium (Fig. 5), confirming previous findings from our group. In addition, the concentration-response curves of SNP in the presence of E and MF fractions demonstrated an endothelium-independent vasorelaxant pathway (Fig. 4), which aligns with studies indicating that NO donors like SNP exert their effects mainly through sGC activation and K^+ channel modulation (Gagov et al., 2022; Rodrigues et al., 2011). Our earlier phytochemical characterization identified compounds **4** and **5** (monodesmosidic triterpene saponins) in the MF fraction, which likely contribute to the vasoconstrictor response through mechanisms involving Ca^{2+} influx via voltage-operated channels and/or α_2-adrenoceptor stimulation (Bareño et al., 2020).

Several studies have reported the antihypertensive properties of oleanolic acid and its derivatives, suggesting a potential involvement of the NO signaling pathway and antioxidant mechanisms (Ayeleso et al., 2017; Pollier and Goossens, 2012; Sultana and Ata, 2008; Zhang et al., 2020). Additionally, oleanolic acid has demonstrated efficacy in preventing cardiac fibrosis (Wang et al., 2023). Overall, the ethanolic extract of

P. quadrangularis contains multiple bioactive compounds with beneficial effects on cardiovascular health, particularly in the context of hypertension (Table 1).

Although the present study provides new insights into the cardiovascular effects of *P. quadrangularis* extract and its fractions, certain aspects warrant further exploration. Future studies should consider the molecular characterization of anti-remodeling pathways, such as the expression of eNOS, iNOS, TGF-β, and collagen I/III in heart and aortic tissues, as well as the assessment of oxidative stress markers (e.g., MDA levels, SOD activity, GSH/GSSG ratio) to confirm the proposed mechanisms. Additionally, long-term treatment protocols would help determine the persistence of the antihypertensive effect and assess potential toxicity. The quantification of key metabolites in plasma via LC-MS/MS could also clarify their bioavailability and contribution to the observed effects. Despite these expansion opportunities, this study presents a significant advancement in understanding the pharmacological potential of *P. quadrangularis*, particularly in the context of hypertension and cardiovascular remodeling.

CONCLUSION

The phytochemical study of *P. quadrangularis* extract allowed the identification of compounds that have not been previously reported. The oral administration of fractions and extract to SHRs attenuated the progression of hypertension, improved aortic and mesenteric relaxations, and decreased cardiac hypertrophy and vascular remodeling, reflected by a significant decrease in interstitial fibrosis and structural changes in cells. The evaluation of fractions in the aortic rings of normotensive rats demonstrated that cGMP, NOS, cholinergic receptors, Ca^{2+} influx via voltage-operated channel activation, or the α_2 adrenoceptor pathway could be implicated in the antihypertensive effect. Although these findings provide valuable insights into the cardiovascular effects of *P. quadrangularis*, further studies are required to elucidate the precise mechanisms underlying its antihypertensive properties.

CONFLICT OF INTEREST

The authors declare no conflicts of interest.

ACKNOWLEDGMENTS

The authors would like to express their sincere gratitude to the Ministry of Science (MinCiencias), Colombia, for the financial support provided through Call No. 727 of 2015 (Code 40174, Hermes, UNCSB). They also extend their thanks to the Department of Pharmaceutical Sciences and the Department of Physiology and Pharmacology, as well as to the faculty of the University of Salamanca, for their valuable technical support throughout this research.

REFERENCES

Al-Akwaa A, Asmawi M, Dewa A, Mahmud R (2020) Antihypertensive activity and vascular reactivity mechanisms of *Vitex pubescens* leaf extracts in spontaneously hypertensive rats. Heliyon 6(7): e04588. https://doi.org/10.1016/j.heliyon.2020.e04588

Álvarez M, Caldiz C, Fantinelli J, Garciareña C, Console G, Chiappe de Cingolani G, Mosca S (2008) Is cardiac hypertrophy in spontaneously hypertensive rats the cause or the consequence of oxidative stress? Hypertens Res 31(7): 1465–1476. https://doi.org/10.1291/hypres.31.1465

Ameen A, Al-Habib O (2021) Vasorelaxant effect of vitexin, procyanidin B2 and isoquercetine on rat's aortic smooth muscle. Technium BioChemMed 2(4): 17–28.

Amina M, Alarfaj N, El-Tohamy M, Musayeib N, Oraby H (2018) Sequential injection-chemiluminescence evaluation of stigmasterol glucoside and luteolin via green synthesis of silver nanoparticles using biomass of *plectranthus asirensis*. Green Chem Lett Rev 11(4): 523–533. https://doi.org/10.1080/17518253.2018.1543457

Ayeleso T, Matumba M, Mukwevho E (2017) Oleanolic acid and its derivatives: Biological activities and therapeutic potential in chronic diseases. Molecules 22(11): 1915. https://doi.org/10.3390/molecules22111915

Bakrim S, Benkhaira N, Bourais I, Benali T, Lee L, El Omari N, Sheikh R, Goh K, Ming L, Bouyahya A (2022) Health benefits and pharmacological properties of stigmasterol. Antioxidants 11(10): 1912. https://doi.org/10.3390/antiox11101912

Bareño L, Puebla P, San Feliciano A, Guerrero M (2020) Vascular mechanisms of triterpenoid saponins isolated from *Passiflora quadrangularis* L. Vitae 27(2): 341585. https://doi.org/10.17533/udea.vitae.v27n2a02

Bareño L, Puebla P, Guerra C, San Feliciano A, Isaza G, Guerrero M (2017) *Passiflora quadrangularis* L. prevents experimental hypertension and vascular remodeling in rats exposed to nitric oxide deficit. Vitae 24(3): 186–195. https://doi.org/10.17533/udea.vitae.v24n4a04

Boateng E, Ampofo A (2023) A glimpse into the future: modelling global prevalence of hypertension. BMC Public Health 23(1): 1906. https://doi.org/10.1186/S12889-023-16662-Z

Castro P, Hoshino A, Campos J, Rieli F (2007) Possible anxiolytic effect of two extracts of *Passiflora quadrangularis* L. in experimental models. Phytother Res 21(5): 481–484. https://doi.org/10.1002/ptr.2079

Che X, Wang X, Zhang J, Peng C, Zhen Y, Shao X, Zhang G, Dong L (2016) Vitexin exerts cardioprotective effect on chronic myocardial ischemia/reperfusion injury in rats via inhibiting myocardial apoptosis and lipid peroxidation. Am J Transl Res 8(8): 3319-3328. https://www.ncbi.nlm.nih.gov/pmc/articles/PMC5009384/

Costa G, Gazola A, Madóglio F, Zucolotto S, Reginatto F, Castellanos L, Ramos F, Duque C, Schenkel E (2013) Vitexin derivates as chemical market in the differentiation of the closely related species *Passiflora alata* Curtis and *Passiflora quadrangularis* Linn. J Liq Chromatogr Relat Technol 36(12): 1697–1707. https://doi.org/10.1080/10826076.2012.695316

Dhawan K, Dhawan S, Sharma A (2004) *Passiflora*: A review update. J Ethnopharmacol 94(1): 1–23. https://doi.org/10.1016/j.jep.2004.02.023

El-Askary H (2005) Terpenoids from *Cleome droserifolia* (Forssk.) Del. Molecules 10(8): 971–977. https://doi.org/10.3390/10080971

Elgendy E, Al-Ghamdy H (2007) Thermal and photooxidation reactions of the steroids: β-sitosterol, stigmasterol and diosgenin. Taiwan Pharm J 59(3): 113–132.

Ferreres F, Gil A, Andrade P, Valentão P, Tomás F (2007) Characterization of C-glycosyl flavones O-glycosylated by liquid chromatography-tandem mass spectrometry. J Chromatogr A 1161(1–2): 214–223. https://doi.org/10.1016/j.chroma.2007.05.103

Finley J, Shahidi F, Finley J (2001) Omega-3 Fatty Acids: Chemistry, Nutrition, and Health Effects. Washington: American Chemical Society. https://pubs.acs.org/doi/10.1021/bk-2001-0788

Fiorim J, Faustino R, Júnior R, Fernades B, Ronacher M, Simão A, Stefanon I, Jesus M, Salaices M, Valentim D (2012) Activation of K^+ channels and Na^+ / K^+ ATPase prevents aortic endothelial dysfunction in 7-day lead-treated rats. Toxicol Appl Pharmacol 262(1): 22–31. https://doi.org/10.1016/j.taap.2012.04.015

Fraser B, Perlmutter P, Wijesundera C (2007) Practical syntheses of triacylglycerol regioisomers containing long-chain polyunsaturated fatty acids. JAOCS 84(1): 11–21. https://doi.org/10.1007/s11746-006-1001-9

Gagov H, Gribkova I, Serebryakov V, Schubert R (2022) Sodium nitroprusside-induced activation of vascular smooth muscle BK channels is mediated by PKG rather than by a direct interaction with NO. Int J Mol Sci 23(5): 2798. https://doi.org/10.3390/ijms23052798

Gao D, Ning N, Hao G, Niu X (2012) Pioglitazone attenuates vascular fibrosis in spontaneously hypertensive rats. PPAR Res 2012: 856426. https://doi.org/10.1155/2012/856426

Gil M, Ferreres F, Tomas F (1998) Effect of modified atmosphere packaging on the flavonoids and vitamin C content of minimally processed Swiss chard (*Beta vulgaris* subspecies *cycla)*. J Agric Food Chem 46(5): 2007–2012. https://doi.org/10.1021/jf970924e

Guillén M, Ruiz A (2003) ^{1}H nuclear magnetic resonance as a fast tool for determining the composition of acyl chains in acylglycerol mixtures. Eur J Lipid Sci Technol 105(9): 502–507. https://doi.org/10.1002/ejlt.200300799

Hawlitschek C, Brendel J, Gabriel P, Schierle K, Salameh A, Zimmer H, Rassler B (2022) Antihypertensive and cardioprotective effects of different monotherapies and combination therapies in young spontaneously hypertensive rats – A pilot study. Saudi J Biol Sci 29(1): 339–345. https://doi.org/10.1016/J.SJBS.2021.08.093

He M, Min J, Kong W, He X, Li J, Peng B (2016) A review on the pharmacological effects of vitexin and isovitexin. Fitoterapia 115: 74–85. https://doi.org/10.1016/j.fitote.2016.09.011

Ingale A, Hivrale A (2010) Pharmacological studies of *Passiflora* sp. and their bioactive compounds. Afr J Plant Sci 4(10): 417–426. https://doi.org/10.5897/AJPS.9000185

Kapoor R, Patil UK (2011) Importance and production of omega-3 fatty acids from natural sources. Int Food Res J 18: 493–499.

Khabazian I, Bains J, Williams D, Cheung J, Wilson J, Pasqualotto B, Pelech S, Andersen R, Wang Y, Liu L, Nagai A, Kim S, Craig U, Shaw C (2002) Isolation of various forms of sterol beta-D-glucoside from the seed of *Cycas circinalis*: Neurotoxicity and implications for ALS-parkinsonism dementia complex. J Neurochem 82(3): 516–528. https://doi.org/10.1046/J.1471-4159.2002.00976.X

Kokubo M, Uemura A, Matsubara T, Murohara T (2005) Noninvasive evaluation of the time course of change in cardiac function in spontaneously hypertensive rats by echocardiography. Hypertens Res 28(7): 601–609. https://doi.org/10.1291/hypres.28.601

Korkmaz S, Loganathan S, Mikles B, Radovits T, Barnucz E, Hirschberg K, Li S., Hegedüs P, Páli S, Weymann A, Karck M, Szabó G (2013) Nitric oxide- and heme-independent activation of soluble guanylate cyclase attenuates peroxynitrite-induced endothelial dysfunction in rat aorta. J Cardiovasc Pharmacol Ther 18(1): 70–77. https://doi.org/10.1177/1074248412455696

Lee D, Noh H, Choi J, Lee K, Lee M, Lee J, Hong Y, Lee S, Kim S, Kim G (2013) Anti-inflammatory cycloartane-type saponins of *Astragalus membranaceus*. Molecules 18(4): 3725–3732. https://doi.org/10.3390/molecules18043725

Lozano R, Naghavi M, Foreman K, Lim S, Shibuya K, Aboyans V, Abraham J, Adair T, Aggarwal R, Ahn S, AlMazroa M, Alvarado M, Anderson H, Anderson L, Andrews K, Atkinson C, Baddour L, Barker S, Bartels D, Murray C (2012) Global and regional mortality from 235 causes of death for 20 age groups in 1990 and 2010: a systematic analysis for the Global Burden of Disease Study 2010. The Lancet 380 (9859): 2095–2128. https://doi.org/10.1016/S0140-6736(12)61728-0

Mali V, Mohan V, Bodhankar S (2012) Antihypertensive and cardioprotective effects of the *Lagenaria siceraria* fruit in N^G-nitro-L-arginine methyl ester (L-NAME) induced hypertensive rats. Pharm Biol 50(11): 1428–1435. https://doi.org/10.3109/13880209.2012.684064

Man S, Gao W, Zhang Y, Huang L, Liu C (2010) Chemical study and medical application of saponins as anti-cancer agents. Fitoterapia 81(7): 703–714. https://doi.org/10.1016/j.fitote.2010.06.004

Martos T, Csabai M, Bagyura Z, Ocsovszky Z, Rafael B, Sallay V, Merkely B (2020) Cardiovascular disease risk perception in a Hungarian community sample: psychometric evaluation of the ABCD Risk Perception Questionnaire. BMJ Open 10(7): e036028. https://doi.org/10.1136/bmjopen-2019-036028

Moloudizargari M, Mikaili P, Aghajanshakeri S, Asghari M, Shayegh J (2013) Pharmacological and therapeutic effects of *Peganum harmala* and its main alkaloids. Pharmacogn Rev 7(14): 199–212. https://doi.org/10.4103/0973-7847.120524

Ngo D, Vo T (2019) An updated review on pharmaceutical properties of gamma-aminobutyric acid. Molecules 24(15): 2678. https://doi.org/10.3390/molecules24152678

Orsini F, Pelizzoni F, Verotta L (1985) Quadranguloside, a cycloartane triterpene glycoside from *Passiflora quadrangularis*. Phytochemistry 25(1): 191–193. https://doi.org/10.1016/S0031-9422(00)94527-8

Orsini F, Pellizzoni F, Ricca G, Verotta L (1987) Triterpene glycosides related to quadranguloside from *Passiflora quadrangularis*. Phytochemistry 26(4): 1101–1105. https://doi.org/10.1016/S0031-9422(00)82358-4

Pollier J, Goossens A (2012) Oleanolic acid. Phytochemistry 77: 10–15. https://doi.org/10.1016/j.phytochem.2011.12.022

Pratiwi R, Nantasenamat C, Ruankham W, Suwanjang W, Prachayasittikul V, Prachayasittikul S, Phopin K (2021) Mechanisms and neuroprotective activities of stigmasterol against oxidative stress-induced neuronal cell death via sirtuin family. Front Nutr 8: 648995. https://doi.org/10.3389/fnut.2021.648995

Rameshrad M, Babaei H, Azarmi Y, Fadaei D (2016) Rat aorta as a pharmacological tool for *in vitro* and *in vivo* studies. Life Sci 145: 190–204. https://doi.org/10.1016/j.lfs.2015.12.043

Reginatto F, Kauffmann C, Schripsema J, Guillaume D, Gosmann G, Schenkef E (2001) Steroidal and triterpenoidal glucosides from *Passiflora alata*. J Braz Chem Soc 12(1): 32–36. https://doi.org/10.1590/S0103-50532001000100003

Rodrigues G, Cicillini S, Silva R, Bendhack (2011) Mechanisms underlying the vascular relaxation induced by a new nitric

oxide generator. Nitric Oxide 25(3): 331–337. https://doi.org/10.1016/j.niox.2011.06.002

Sakalem E, Negri G, Tabach R (2011) Chemical composition of hydroethanolic extracts from five species of the *Passiflora* genus. Rev Bras Farmacogn *22*(6): 1219–1232. https://doi.org/10.1590/S0102-695X2012005000108

Sánchez D, Kassan M, Contreras M, Carrón R, Recio I, Montero M, Sevilla M (2011) Long-term intake of a milk casein hydrolysate attenuates the development of hypertension and involves cardiovascular benefits. Pharmacol Res 63(5): 398–404. https://doi.org/10.1016/j.phrs.2011.01.015

Sen A (2020) Prophylactic and therapeutic roles of oleanolic acid and its derivatives in several diseases. World J Clin Cases 8(10): 1767-1792. https://doi.org/10.12998/wjcc.v8.i10.1767

Sepúlveda P, Costa G, Aragón D, Ramos F, Castellanos L (2018) Analysis of vitexin in aqueous extracts and commercial products of Andean *Passiflora* species by UHPLC-DAD. J App Pharm Sci 8(9): 81–86. https://doi.org/10.7324/japs.2018.8912

Shi C, Chen S, Wang G, Liao J, Chen C (2000). Vasorelaxant effect of harman. Eur J Pharmacol 390(3): 319–325. https://doi.org/10.1016/S0014-2999(99)00928-0

Song Y, Yu J, Song J, Wang S, Cao T, Liu Z, Gao X, Wei Y (2021) The antihypertensive effect and mechanisms of bioactive peptides from *Ruditapes philippinarum* fermented with *Bacillus natto* in spontaneously hypertensive rats. J Funct Foods 79: 104411. https://doi.org/10.1016/j.jff.2021.104411

Sultana N, Ata A (2008) Oleanolic acid and related derivatives as medicinally important compounds. J Enzyme Inhib Med Chem *23*(6): 739–756. https://doi.org/10.1080/14756360701633187

Tangsucharit P, Takatori S, Zamami Y, Goda M (2016) Muscarinic acetylcholine receptor M1 and M3 subtypes mediate acetylcholine-induced endothelium-independent vasodilatation in rat mesenteric arteries. J Pharmacol Sci 130(1): 24–32. https://doi.org/10.1016/j.jphs.2015.12.005

Wang A, Ma H, Yi Y, Zhu S, Yu Z, Zhu J, Mei S, Bahetibike S, Lu Y, Huang L, Yang R, Wang R, Xiao S, Qi R (2023) Oleanolic acid derivative alleviates cardiac fibrosis through inhibiting PTP1B activity and regulating AMPK/TGF-β/Smads pathway. Eur J Pharmacol 960: 176116. https://doi.org/10.1016/j.ejphar.2023.176116

Wang C, Xu F, Shang J, Xiao H, Fan W, Dong F, Hu J, Zhou J (2013) Cycloartane triterpenoid saponins from water soluble of *Passiflora edulis* Sims and their antidepressant-like effects. J Ethnopharmacol 148(3): 812–817. https://doi.org/10.1016/j.jep.2013.05.010

Yang C, Kandaswamy V, Young D, Sen S (1997) Changes in collagen phenotypes during progression and regression of cardiac hypertrophy. Cardiovasc Res 36(2): 236–245. https://doi.org/10.1016/S0008-6363(97)00186-7

Zahmanov G, Alipieva K, Simova S, Georgiev M (2015) Metabolic differentiations of dwarf elder by NMR-based metabolomics. Phytochem Lett 11: 404–409. https://doi.org/10.1016/j.phytol.2014.11.021

Zanetti M, Gortan G, Burekovic I, Barazzoni R (2010) Caloric restriction improves endothelial dysfunction during vascular aging: Effects on nitric oxide synthase isoforms and oxidative stress in rat aorta. Exp Gerontol 45(11): 848–855. https://doi.org/10.1016/j.exger.2010.07.002

Zeng Y, Zhang Y, Weng Q, Hu M, Zhong G (2010) Cytotoxic and insecticidal activities of derivatives of harmine, a natural insecticidal component isolated from *Peganum harmala*. Molecules 15(11): 7775–7791. https://doi.org/10.3390/molecules15117775

Zhang H, Zhang R, LiaoX, Yang D, Wang Y, Zhao Y, Xu G, Liu C, Li Y, Liao S, Zhou M (2021) Discovery of β-carboline derivatives as a highly potent cardioprotectant against myocardial ischemia-reperfusion injury. J Med Chem 64(13): 9166–9181. https://doi.org/10.1021/acs.jmedchem.1c00384

Zhang P, Li D, Zhu J, Hu J (2023) Antihypertensive effects of *Pleurospermum lindleyanum* aqueous extract in spontaneously hypertensive rats. J Ethnopharmacol 308: 116261. https://doi.org/10.1016/j.jep.2023.116261

Zhang S, Liu Y, Wang X, Tian Z, Qi D, Li Y, Jiang H (2020) Antihypertensive activity of oleanolic acid is mediated via downregulation of secretory phospholipase A2 and fatty acid synthase in spontaneously hypertensive rats. Int J Mol Med 46(6): 2019–2034. https://doi.org/10.3892/ijmm.2020.4744

AUTHOR CONTRIBUTION:

Contribution	Bareño LL	Guerrero MF	Puebla P	Montero MJ	Sevilla MA	San Feliciano A
Concepts or ideas	x	x	x	x	x	x
Design	x	x	x	x	x	x
Definition of intellectual content	x	x				
Literature search	x		x			
Experimental studies	x	x	x	x	x	
Data acquisition	x		x	x	x	
Data analysis	x	x	x	x	x	x
Statistical analysis	x	x	x	x	x	
Manuscript preparation	x					
Manuscript editing	x	x	x	x	x	x
Manuscript review	x	x	x	x	x	x

Citation Format: Bareño LL, Guerrero MF, Puebla P, Montero MJ, Sevilla MA, San Feliciano A (2025) Phytochemical analysis of *Passiflora quadrangularis* L. and its potential role in hypertension and cardiac remodeling. J Pharm Pharmacogn Res 13(6): 1649–1677. https://doi.org/10.56499/jppres24.2213_13.6.1649

Publisher's Note: All claims expressed in this article are solely those of the authors and do not necessarily represent those of their affiliated organizations, or those of the publisher, the editors and the reviewers. Any product that may be evaluated in this article, or claim that may be made by its manufacturer, is not guaranteed or endorsed by the publisher.

Open Access: This article is distributed under the terms of the Creative Commons Attribution 4.0 International License (http://creativecommons.org/licenses/by/4.0/), which permits use, duplication, adaptation, distribution and reproduction in any medium or format, as long as you give appropriate credit to the original author(s) and the source, provide a link to the Creative Commons license and indicate if changes were made.

Supplementary Data

Table SM1. E_{max} and pEC_{50} of ACh, SNP and PE in aortic and mesenteric rings of E, DF, MF and C groups.

Aortic rings						
Compound/ fraction	**ACh**		**SNP**		**PE**	
	E_{max} (%)	**pEC_{50}**	**E_{max} (%)**	**pEC_{50}**	**E_{max} (%)**	**EC_{50}**
C	57.0 ± 8.2	7.06 ± 0.04	95.0 ± 0.3	7.90 ± 0.02	96.0 ± 0.8	6.73 ± 0.03
E	77.0 ± 0.6*	7.55 ± 0.03*	96.0 ± 0.4	7.52 ± 0.02*	112.0 ± 1.4	6.80 ± 0.04
DF	76.0 ± 0.4*	7.76 ± 0.02*	91.0 ± 0.6	7.32 ± 0.03*	88.0 ± 1.0	7.00 ± 0.04*
MF	76.0 ± 0.5*	7.38 ± 0.02*	95.0 ± 0.5	7.89 ± 0.03	109.0 ± 0.8	6.72 ± 0.03*
Mesenteric rings						
Compound/ fraction	**ACh**		**SNP**		**PE**	
	E_{max} (%)	**pEC_{50}**	**E_{max} (%)**	**pEC_{50}**	**E_{max} (%)**	**EC_{50}**
C	70.0 ± 0.6	7.88 ± 0.03	84.0 ± 0.9	7.93 ± 0.06	171.0 ± 1.9	5.56 ± 0.02
E	85.0 ± 0.5*	7.90 ± 0.02*	87.0 ± 0.6	7.70 ± 0.03	257.0 ± 8.2	5.65 ± 0.07
DF	83.0 ± 0.5*	8.23 ± 0.03*	85.0 ± 0.7	7.22 ± 0.03*	236.0 ± 6.9	5.58 ± 0.06
MF	83.0 ± 0.5*	8.08 ± 0.03*	84.0 ± 0.7	7.31 ± 0.04*	167.0 ± 3.2	5.40 ± 0.04

The results are expressed as mean ± SEM of the number of dates of 5 animals per treatment. pCE_{50}(-logCE_{50}, g/mL) and E_{max} (percent of 0.1 µM and 3 µM aorta and mesenteric rings, respectively, PE maximal contraction). Units for pCE_{50} are expressed as M. *p<0.05 vs. C. C: control; E: Total extract of *P. quadrangularis*; DF: CH_2Cl_2 fraction; MF: MeOH fraction.

Table SM2. Morphometric parameters of the heart and aorta SHR**.**

Heart				
Morphometric parameters	**C**	**E**	**DF**	**MF**
CH (mg/g)	3.02 ± 0.08	3.03 ± 0.03	3.09 ± 0.03	3.03 ± 0.05
W_{IVS}/R (mm)	0.58 ± 0.04	0.58 ± 0.01	0.55 ± 0.01	0.54 ± 0.01
W_{LV}/R (mm)	0.74 ± 0.03	0.62 ± 0.04	0.57 ± 0.30*	0.60 ± 0.01
Aorta				
CSA (mm)	0.58 ± 0.02	0.59 ± 0.01	0.61 ± 0.01	0.60 ± 0.01
W_m/L (mm)	0.09 ± 0.00	0.07 ± 0.00	0.07 ± 0.00	0.07 ± 0.00

The results are expressed as mean ± SEM of the number of dates of 5 animals per treatment. *p<0.05 vs. C.

Total extract of *P. quadrangularis* (E), soluble CH_2Cl_2 fraction (DF), soluble MeOH fraction (MF), and control (C) (75 mg/kg/day). CH: cardiac hypertrophy, W_{IVS}/R: thickness of the interventricular septum/ heart radius ratio, W_{LV}/R: left ventricular thickness/heart radius ratio, CSA_m: Sectional area of the middle layer, and W_m/L: middle layer thickness/lumen ratio.

2way ANOVA
Multiple comparisons

1	Within each row, compare columns (simple effects within rows)				
2					
3	Number of families	7			
4	Number of comparisons per family	3			
5	Alpha	0.05			
6					
7	Bonferroni's multiple comparisons test	Mean Diff.	95% CI of diff.	Significant?	Summary
8					
9	Row 1				
10	E vs. C	0.2000	-11.64 to 12.04	No	ns
11	Fs vs. C	1.400	-10.44 to 13.24	No	ns
12	Fi vs. C	-3.000	-14.84 to 8.838	No	ns
13					
14	Row 2				
15	E vs. C	-23.40	-35.24 to -11.56	Yes	****
16	Fs vs. C	-21.20	-33.04 to -9.362	Yes	****
17	Fi vs. C	-16.60	-28.44 to -4.762	Yes	**
18					
19	Row 3				
20	E vs. C	-24.40	-36.24 to -12.56	Yes	****
21	Fs vs. C	-18.80	-30.64 to -6.962	Yes	***
22	Fi vs. C	-15.60	-27.44 to -3.762	Yes	**
23					
24	Row 4				
25	E vs. C	-31.20	-43.04 to -19.36	Yes	****
26	Fs vs. C	-26.40	-38.24 to -14.56	Yes	****
27	Fi vs. C	-21.60	-33.44 to -9.762	Yes	****
28					
29	Row 5				
30	E vs. C	-23.60	-35.44 to -11.76	Yes	****
31	Fs vs. C	-28.60	-40.44 to -16.76	Yes	****
32	Fi vs. C	-24.60	-36.44 to -12.76	Yes	****
33					
34	Row 6				
35	E vs. C	-25.60	-37.44 to -13.76	Yes	****
36	Fs vs. C	-31.20	-43.04 to -19.36	Yes	****
37	Fi vs. C	-29.00	-40.84 to -17.16	Yes	****
38					
39	Row 7				
40	E vs. C	-34.40	-46.24 to -22.56	Yes	****
41	Fs vs. C	-38.00	-49.84 to -26.16	Yes	****
42	Fi vs. C	-39.80	-51.64 to -27.96	Yes	****

2way ANOVA
Tabular results

1	Table Analyzed	Presión				
2						
3	Two-way ANOVA	Ordinary				
4	Alpha	0.05				
5						
6	Source of Variation	% of total variation	P value	P value summary	Significant?	
7	Interaction	13.87	< 0.0001	****	Yes	
8	Row Factor	10.25	< 0.0001	****	Yes	
9	Column Factor	50.89	< 0.0001	****	Yes	
10						
11	ANOVA table	SS	DF	MS	F (DFn, DFd)	P value
12	Interaction	3686	18	204.8	F (18, 112) = 3.453	P < 0.0001
13	Row Factor	2726	6	454.3	F (6, 112) = 7.659	P < 0.0001
14	Column Factor	13526	3	4509	F (3, 112) = 76.02	P < 0.0001
15	Residual	6643	112	59.31		
16						
17	Number of missing values	0				

Figure SM1. Screenshot of the two-way ANOVA with Bonferroni's multiple comparisons test performed in GraphPad Prism for systolic blood pressure measurements in SHR rats.

Col. stats	A C Y	B E Y	C Fi Y	D Fs Y
1 Number of values	22	20	20	20
2				
3 Minimum	406.0	706.0	423.0	618.0
4 25% Percentile	827.8	961.3	750.8	993.0
5 Median	1022	1141	905.5	1103
6 75% Percentile	1289	1353	1064	1516
7 Maximum	1791	1853	1194	1736
8				
9 Mean	1076	1181	873.3	1174
10 Std. Deviation	401.8	288.3	231.6	332.4
11 Std. Error of Mean	85.67	64.47	51.80	74.33
12				
13 Lower 95% CI of mean	898.2	1046	764.9	1018
14 Upper 95% CI of mean	1255	1316	981.7	1329
15				
16 Sum	23680	23614	17466	23473

Figure SM2. Screenshot of the column statistics (Col. stats) output from GraphPad Prism, showing the initial contraction values of aortic rings from SHR rats pre-contracted with phenylephrine (0.1 µM), prior to treatment administration.

1way ANOVA
ANOVA

1	Table Analyzed	PE mg -ACh				
2						
3	ANOVA summary					
4	F	3.959				
5	P value	0.0111				
6	P value summary	*				
7	Are differences among means statistically significant? (P < 0.05)	Yes				
8	R square	0.1321				
9						
10	Brown-Forsythe test					
11	F (DFn, DFd)	1.187 (3, 78)				
12	P value	0.3201				
13	P value summary	ns				
14	Significantly different standard deviations? (P < 0.05)	No				
15						
16	Bartlett's test					
17	Bartlett's statistic (corrected)	6.091				
18	P value	0.1073				
19	P value summary	ns				
20	Significantly different standard deviations? (P < 0.05)	No				
21						
22	ANOVA table	SS	DF	MS	F (DFn, DFd)	P value
23	Treatment (between columns)	1.232e+006	3	410567	F (3, 78) = 3.959	P = 0.0111
24	Residual (within columns)	8.089e+006	78	103707		
25	Total	9.321e+006	81			
26						
27	Data summary					
28	Number of treatments (columns)	4				
29	Number of values (total)	82				

1way ANOVA
Multiple comparisons

1	Number of families	1							
2	Number of comparisons per family	3							
3	Alpha	0.05							
4									
5	Dunnett's multiple comparisons test	Mean Diff.	95% CI of diff.	Significant?	Summary				
6									
7	C vs. E	-104.3	-342.7 to 134.0	No	ns				
8	C vs. Fi	203.1	-35.31 to 441.4	No	ns				
9	C vs. Fs	-97.29	-335.7 to 141.1	No	ns				
10									
11									
12	Test details	Mean 1	Mean 2	Mean Diff.	SE of diff.	n1	n2	q	DF
13									
14	C vs. E	1076	1181	-104.3	99.50	22	20	1.049	78
15	C vs. Fi	1076	873.3	203.1	99.50	22	20	2.041	78
16	C vs. Fs	1076	1174	-97.29	99.50	22	20	0.9778	78

Figure SM3. Screenshot of the one-way ANOVA analysis with Dunnett's multiple comparisons test performed in GraphPad Prism on aortic rings from SHR rats.

Col. stats

		A	B	C	D
		C	E	Fs	Fi
		Y	Y	Y	Y
1	Number of values	17	19	17	19
2					
3	Minimum	0.4100	0.8200	0.4100	0.5000
4	25% Percentile	1.050	1.620	0.9750	1.690
5	Median	2.150	2.450	2.610	2.730
6	75% Percentile	3.000	3.490	3.710	3.510
7	Maximum	4.900	4.320	8.030	6.950
8					
9	Mean	2.170	2.538	2.837	2.921
10	Std. Deviation	1.225	1.147	2.311	1.688
11	Std. Error of Mean	0.2972	0.2631	0.5605	0.3873
12					
13	Lower 95% CI of mean	1.540	1.985	1.649	2.107
14	Upper 95% CI of mean	2.800	3.091	4.025	3.735
15					
16	Sum	36.89	48.22	48.23	55.50

Figure SM4. Screenshot of the column statistics (Col. stats) output from GraphPad Prism, showing the initial contraction values of mesenteric rings from SHR rats pre-contracted with phenylephrine (3 µM), prior to treatment administration.

1way ANOVA
ANOVA

1	Table Analyzed	PE - ACh				
2						
3	ANOVA summary					
4	F	0.7489				
5	P value	0.5268				
6	P value summary	ns				
7	Are differences among means statistically significant? (P < 0.05)	No				
8	R square	0.03198				
9						
10	Brown-Forsythe test					
11	F (DFn, DFd)	2.066 (3, 68)				
12	P value	0.1129				
13	P value summary	ns				
14	Significantly different standard deviations? (P < 0.05)	No				
15						
16	Bartlett's test					
17	Bartlett's statistic (corrected)	10.51				
18	P value	0.0147				
19	P value summary	*				
20	Significantly different standard deviations? (P < 0.05)	Yes				
21						
22	ANOVA table	SS	DF	MS	F (DFn, DFd)	P value
23	Treatment (between columns)	6.093	3	2.031	F (3, 68) = 0.7489	P = 0.5268
24	Residual (within columns)	184.4	68	2.712		
25	Total	190.5	71			
26						
27	Data summary					
28	Number of treatments (columns)	4				
29	Number of values (total)	72				

1way ANOVA
Multiple comparisons

1	Number of families	1							
2	Number of comparisons per family	3							
3	Alpha	0.05							
4									
5	Dunnett's multiple comparisons test	Mean Diff.	95% CI of diff.	Significant?	Summary				
6									
7	C vs. E	-0.3679	-1.689 to 0.9532	No	ns				
8	C vs. Fs	-0.6671	-2.024 to 0.6902	No	ns				
9	C vs. Fi	-0.7511	-2.072 to 0.5700	No	ns				
10									
11									
12	Test details	Mean 1	Mean 2	Mean Diff.	SE of diff.	n1	n2	q	DF
13									
14	C vs. E	2.170	2.538	-0.3679	0.5498	17	19	0.6691	68
15	C vs. Fs	2.170	2.837	-0.6671	0.5649	17	17	1.181	68
16	C vs. Fi	2.170	2.921	-0.7511	0.5498	17	19	1.366	68

Figure SM5. Screenshot of the one-way ANOVA analysis with Dunnett's multiple comparisons test performed in GraphPad Prism on aortic rings from SHR rats.

1way ANOVA
ANOVA

1	Table Analyzed	ACh				
2						
3	Repeated measures ANOVA summary					
4	Assume sphericity?	No				
5	F	63.04				
6	P value	< 0.0001				
7	P value summary	****				
8	Statistically significant (P < 0.05)?	Yes				
9	Geisser-Greenhouse's epsilon	0.6887				
10	R square	0.8874				
11						
12	Was the matching effective?					
13	F	134.0				
14	P value	< 0.0001				
15	P value summary	****				
16	Is there significant matching (P < 0.05)?	Yes				
17	R square	0.8341				
18						
19	ANOVA table	SS	DF	MS	F (DFn, DFd)	P value
20	Treatment (between columns)	3525	3	1175	F (2.066, 16.53) = 63.04	P < 0.0001
21	Individual (between rows)	19980	8	2498	F (8, 24) = 134.0	P < 0.0001
22	Residual (random)	447.4	24	18.64		
23	Total	23953	35			
24						
25	Data summary					
26	Number of treatments (columns)	4				
27	Number of subjects (rows)	9				

1way ANOVA
Multiple comparisons

1	Number of families	1							
2	Number of comparisons per family	6							
3	Alpha	0.05							
4									
5	Bonferroni's multiple comparisons test	Mean Diff.	95% CI of diff.	Significant?	Summary				
6									
7	C vs. E	-22.46	-30.04 to -14.89	Yes	****				
8	C vs. Fs	-25.68	-34.17 to -17.20	Yes	****				
9	C vs. Fi	-16.58	-24.27 to -8.894	Yes	***				
10	E vs. Fs	-3.219	-7.389 to 0.9507	No	ns				
11	E vs. Fi	5.879	0.9206 to 10.84	Yes	*				
12	Fs vs. Fi	9.098	0.7117 to 17.48	Yes	*				
13									
14									
15	Test details	Mean 1	Mean 2	Mean Diff.	SE of diff.	n1	n2	t	DF
16									
17	C vs. E	30.22	52.68	-22.46	2.177	9	9	10.32	8
18	C vs. Fs	30.22	55.90	-25.68	2.438	9	9	10.53	8
19	C vs. Fi	30.22	46.80	-16.58	2.211	9	9	7.502	8
20	E vs. Fs	52.68	55.90	-3.219	1.199	9	9	2.686	8
21	E vs. Fi	52.68	46.80	5.879	1.425	9	9	4.125	8
22	Fs vs. Fi	55.90	46.80	9.098	2.411	9	9	3.774	8

Figure SM6. Screenshot of the one-way ANOVA followed by Bonferroni's multiple comparisons test performed in GraphPad Prism for the concentration–response curves to acetylcholine (ACh) in aortic rings from SHR rats.

1way ANOVA
ANOVA

1	Table Analyzed	ACh				
2						
3	Repeated measures ANOVA summary					
4	Assume sphericity?	No				
5	F	31.70				
6	P value	< 0.0001				
7	P value summary	****				
8	Statistically significant (P < 0.05)?	Yes				
9	Geisser-Greenhouse's epsilon	0.6828				
10	R square	0.7985				
11						
12	Was the matching effective?					
13	F	279.1				
14	P value	< 0.0001				
15	P value summary	****				
16	Is there significant matching (P < 0.05)?	Yes				
17	R square	0.9494				
18						
19	ANOVA table	SS	DF	MS	F (DFn, DFd)	P value
20	Treatment (between columns)	1075	3	358.2	F (2.048, 16.39) = 31.70	P < 0.0001
21	Individual (between rows)	25236	8	3155	F (8, 24) = 279.1	P < 0.0001
22	Residual (random)	271.2	24	11.30		
23	Total	26582	35			
24						
25	Data summary					
26	Number of treatments (columns)	4				
27	Number of subjects (rows)	9				

1way ANOVA
Multiple comparisons

1	Number of families	1							
2	Number of comparisons per family	3							
3	Alpha	0.05							
4									
5	Bonferroni's multiple comparisons test	Mean Diff.	95% CI of diff.	Significant?	Summary				
6									
7	C vs. E	-11.61	-16.07 to -7.157	Yes	***				
8	C vs. Fs	-12.83	-19.21 to -6.455	Yes	***				
9	C vs. Fi	-13.19	-16.45 to -9.938	Yes	****				
10									
11									
12	Test details	Mean 1	Mean 2	Mean Diff.	SE of diff.	n1	n2	t	DF
13									
14	C vs. E	48.78	60.39	-11.61	1.477	9	9	7.861	8
15	C vs. Fs	48.78	61.61	-12.83	2.114	9	9	6.069	8
16	C vs. Fi	48.78	61.97	-13.19	1.080	9	9	12.22	8

Figure SM7. Screenshot of the one-way ANOVA followed by Bonferroni's multiple comparisons test performed in GraphPad Prism for the concentration–response curves to acetylcholine (ACh) in mesenteric rings from SHR rats.

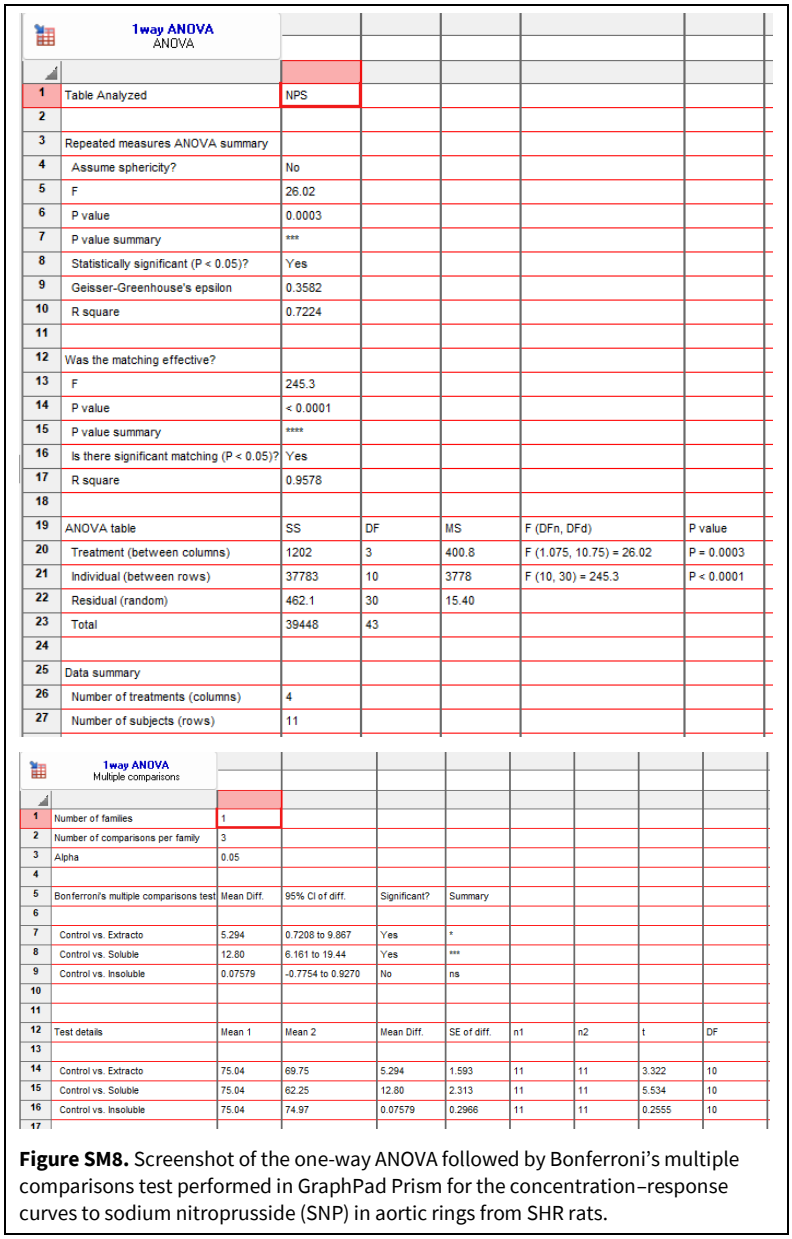

1way ANOVA
ANOVA

1	Table Analyzed	NPS				
2						
3	Repeated measures ANOVA summary					
4	Assume sphericity?	No				
5	F	26.02				
6	P value	0.0003				
7	P value summary	***				
8	Statistically significant (P < 0.05)?	Yes				
9	Geisser-Greenhouse's epsilon	0.3582				
10	R square	0.7224				
11						
12	Was the matching effective?					
13	F	245.3				
14	P value	< 0.0001				
15	P value summary	****				
16	Is there significant matching (P < 0.05)?	Yes				
17	R square	0.9578				
18						
19	ANOVA table	SS	DF	MS	F (DFn, DFd)	P value
20	Treatment (between columns)	1202	3	400.8	F (1.075, 10.75) = 26.02	P = 0.0003
21	Individual (between rows)	37783	10	3778	F (10, 30) = 245.3	P < 0.0001
22	Residual (random)	462.1	30	15.40		
23	Total	39448	43			
24						
25	Data summary					
26	Number of treatments (columns)	4				
27	Number of subjects (rows)	11				

1way ANOVA
Multiple comparisons

1	Number of families	1							
2	Number of comparisons per family	3							
3	Alpha	0.05							
4									
5	Bonferroni's multiple comparisons test	Mean Diff.	95% CI of diff.	Significant?	Summary				
6									
7	Control vs. Extracto	5.294	0.7208 to 9.867	Yes	*				
8	Control vs. Soluble	12.80	6.161 to 19.44	Yes	***				
9	Control vs. Insoluble	0.07579	-0.7754 to 0.9270	No	ns				
10									
11									
12	Test details	Mean 1	Mean 2	Mean Diff.	SE of diff.	n1	n2	t	DF
13									
14	Control vs. Extracto	75.04	69.75	5.294	1.593	11	11	3.322	10
15	Control vs. Soluble	75.04	62.25	12.80	2.313	11	11	5.534	10
16	Control vs. Insoluble	75.04	74.97	0.07579	0.2966	11	11	0.2555	10
17									

Figure SM8. Screenshot of the one-way ANOVA followed by Bonferroni's multiple comparisons test performed in GraphPad Prism for the concentration–response curves to sodium nitroprusside (SNP) in aortic rings from SHR rats.

1way ANOVA
ANOVA

1	Table Analyzed	NTP				
2						
3	Repeated measures ANOVA summary					
4	Assume sphericity?	No				
5	F	12.95				
6	P value	0.0033				
7	P value summary	**				
8	Statistically significant (P < 0.05)?	Yes				
9	Geisser-Greenhouse's epsilon	0.3768				
10	R square	0.5643				
11						
12	Was the matching effective?					
13	F	156.7				
14	P value	< 0.0001				
15	P value summary	****				
16	Is there significant matching (P < 0.05)?	Yes				
17	R square	0.9579				
18						
19	ANOVA table	SS	DF	MS	F (DFn, DFd)	P value
20	Treatment (between columns)	878.7	3	292.9	F (1.130, 11.30) = 12.95	P = 0.0033
21	Individual (between rows)	35434	10	3543	F (10, 30) = 156.7	P < 0.0001
22	Residual (random)	678.5	30	22.62		
23	Total	36992	43			
24						
25	Data summary					
26	Number of treatments (columns)	4				
27	Number of subjects (rows)	11				

1way ANOVA
Multiple comparisons

1	Number of families	1							
2	Number of comparisons per family	3							
3	Alpha	0.05							
4									
5	Bonferroni's multiple comparisons test	Mean Diff.	95% CI of diff.	Significant?	Summary				
6									
7	C vs. E	1.968	-1.840 to 5.775	No	ns				
8	C vs. Fs	10.56	1.609 to 19.50	Yes	*				
9	C vs. Fi	8.916	1.719 to 16.11	Yes	*				
10									
11									
12	Test details	Mean 1	Mean 2	Mean Diff.	SE of diff.	n1	n2	t	DF
13									
14	C vs. E	66.59	64.63	1.968	1.327	11	11	1.483	10
15	C vs. Fs	66.59	56.04	10.56	3.117	11	11	3.386	10
16	C vs. Fi	66.59	57.68	8.916	2.508	11	11	3.555	10

Figure SM9. Screenshot of the one-way ANOVA followed by Bonferroni's multiple comparisons test performed in GraphPad Prism for the concentration–response curves to sodium nitroprusside (SNP) in mesenteric rings from SHR rats.

	Paired t test	
1	Table Analyzed	Fr.metanólica
2		
3	Column B	FM -
4	vs.	vs.
5	Column A	FM
6		
7	Paired t test	
8	P value	0.4725
9	P value summary	ns
10	Significantly different (P < 0.05)?	No
11	One- or two-tailed P value?	Two-tailed
12	t, df	t=0.7499 df=9
13	Number of pairs	10
14		
15	How big is the difference?	
16	Mean of differences	-1.641
17	SD of differences	6.919
18	SEM of differences	2.188
19	95% confidence interval	-6.59 to 3.309
20	R squared (partial eta squared)	0.05881
21		
22	How effective was the pairing?	
23	Correlation coefficient (r)	0.9845
24	P value (one tailed)	<0.0001
25	P value summary	****
26	Was the pairing significantly effective?	Yes

Figure SM10. Screenshot of the paired t-test performed in GraphPad Prism for the concentration–response curves to MF in isolated aortic rings from Wistar rats, with and without endothelium.